National Institute for Public Health
and the Environment
Ministry of Health, Welfare and Sport

Fires caused by heat radiation - a method of determining fire focus areas

RIVM report 2024-0149
E. Bloem | P.A.M. Uijt de Haag

Fires caused by heat radiation - a method of determining fire focus areas

RIVM report 2024-0149

Colophon

DOI 10.21945/RIVM-2024-0149

E. Bloem (author), RIVM
P.A.M. Uijt de Haag (author), RIVM

Contact:
omgevingsveiligheid@rivm.nl

This investigation was performed by order, and for the account, of the Ministry of Infrastructure and Water management within the framework of the project M/260119/24/OO

Published by:
National Institute for Public Health and the Environment, RIVM
PO Box 1 | 3720 BA Bilthoven
The Netherlands
www.rivm.nl/en

Synopsis

Fires caused by heat radiation - a method of determining fire focus areas

The heat of a fire can also set fire to buildings in the area. A so-called fire focus area is therefore determined around activities with large quantities of flammable substances. Within this area, people in a building or home may not be adequately protected if additional measures are not taken.

The size of a fire focus area is calculated. This allows the government to consider whether the risks are acceptable or whether measures are necessary. This information is important, for example, for applying for permits to expand a factory or a residential area.

Research by RIVM shows that another method can calculate the focus area more realistically. This new method takes into account both the intensity of the heat of a fire and its duration. This gives the government a better picture of the possible dangers of fires with flammable substances.

The boundary of a fire focus area is determined by the distance at which buildings can catch fire due to a fire. This is calculated with the 'heat radiation'. The heat radiation is highest at the fire itself and decreases the further away you are from it. It takes a while before a fire starts. The higher the heat radiation, the faster the fire will start further away. If a fire lasts for a short time, no fires will start further down. That is why it is important to also include the duration of the fire in the calculation.

The new method makes a big difference in situations where the heat radiation of a fire is initially very high, but soon drops. This is the case, for example, in the event of a burst of a high-pressure natural gas pipeline. The fire focus areas that have been calculated for this so far were too large, requiring unnecessary measures. In fires where the differences in heat radiation are less significant, the fire focus areas remain about the same.

Keywords: secondary fires, heat radiation, piloted ignition, dose relationship, focus area

Publiekssamenvatting

Branden die door warmtestraling ontstaan - een methode om brandaandachtsgebieden te bepalen

Door de hitte van een brand kunnen ook gebouwen in de omgeving in brand komen te staan. Rond activiteiten met grote hoeveelheden ontvlambare stoffen wordt daarom een zogeheten brandaandachts-gebied bepaald. Binnen dit gebied kunnen mensen in een gebouw of woning mogelijk niet genoeg beschermd zijn als er geen extra maatregelen worden genomen.

De grootte van een brandaandachtsgebied wordt berekend. Hiermee kan de overheid afwegen of de risico's acceptabel zijn of dat maatregelen nodig zijn. Deze informatie is bijvoorbeeld belangrijk voor de aanvraag van vergunningen om een fabriek of een woonwijk uit te breiden.

Uit onderzoek van het RIVM blijkt dat een andere methode het aandachtsgebied realistischer kan berekenen. Deze nieuwe methode houdt rekening met zowel de intensiteit van de hitte van een brand als de duur ervan. Hiermee krijgt de overheid een beter beeld van de mogelijke gevaren van branden met ontvlambare stoffen.

De grens van een brandaandachtsgebied wordt bepaald door de afstand waarop gebouwen door een brand vlam kunnen vatten. Dat wordt berekend met de 'warmtestraling'. De warmtestraling is het hoogst bij de brand zelf en neemt af naarmate je er verder weg van staat. Het duurt wel even voordat een brand ontstaat. Hoe hoger de warmte-straling, hoe sneller de brand verderop zal ontstaan. Als een brand kort duurt, ontstaan er verderop geen branden. Daarom is het belangrijk ook de duur van de brand mee te nemen in de berekening.

De nieuwe methode maakt een groot verschil bij situaties waar de warmtestraling van een brand eerst heel hoog is, maar al snel daalt. Dit is bijvoorbeeld het geval bij een breuk van een hogedruk aardgasleiding. De brandaandachtsgebieden die daar tot nu toe voor zijn berekend waren te groot, waardoor onnodig veel maatregelen nodig waren. Bij branden waar de verschillen in de warmtestraling minder groot zijn, blijven de brandaandachtsgebieden ongeveer hetzelfde.

Kernwoorden: brandaandachtsgebied, warmtestraling, dosisbenadering, warmtestralingsdosis, branden, ontsteking

Contents

Summary

In the Netherlands, focus areas were introduced around activities with dangerous substances. A focus area is defined as the effect zone where an incident can have life-threatening consequences for people inside buildings. There are three different focus areas, for toxic clouds, explosions (overpressure) and fire (heat radiation). Focus areas help policymakers to decide whether additional protective measures are needed.

The fire focus area is currently limited to the area with a heat flux of 10 kW/m^2 or more, independently of the duration of the heat flux. For fires in which the heat flux decreases significantly over time this can result in unrealistically large areas of attention. In this report the use of a dose relationship to determine the limits of the fire focus area is investigated.

In this report we investigated the possible effects of industrial fires. Secondary fires, where materials ignite due to the heat radiation of the original fire, require the lowest heat dose and are therefore the primary threat. Other effects such as building collapse and too high temperature inside buildings require a higher radiation dose and were not considered.

Experimental data about the time to ignition for different radiation levels was collected for materials that can be found in and around buildings. This resulted in over 600 datapoints. The dose relationship $\int (R(t) - C)^B dt = A$ was used, where R is the heat flux [kW/m^2], C the critical heat flux [kW/m^2], B a factor [-], t the time [s], and A the reference dose at which piloted ignition occurs [s·(kW/m^2)^B]. These parameters (A, B and C) can be determined by fitting this dose relationship to measurements where the time to ignition was determined for various heat fluxes.

The fit of the dose response relationship to the experimental data resulted in B = 2 and a range of possible values for A and C. The dose relationship was then calibrated against the fire damage due to heat radiation for four incidents with high pressure natural gas pipelines (San Bruno, Sissonville, Ludwigshafen and Danville). This distance was compared with the heat dose as calculated using Safeti-NL, using the characteristics of the pipeline as described in the accident reports. As a result, it was concluded that the best approach uses C = 5 kW/m^2 and A = 28150 s·(kW/m^2)^2.

For a number of example situations, the distance to the boundary of the fire focus area has been calculated using both the 10 kW/m^2 limit and the proposed dose relationship. For pipelines, where the radiation level is very high immediately after the rupture but then drops rapidly, the focus area becomes much smaller. For pool and jet fires, the focus areas are between 2% smaller and 5% larger.

1 Introduction

In the Netherlands, Quantitative Risk Assessment (QRA) is used for decisions on land use planning around sites with dangerous substances. Two measures are used, Individual Risk (IR) and, until 2024, Societal Risk (SR).[1] From 2024 onwards the calculation of Societal Risk has been replaced with the concept of focus areas. A focus area is defined as the effect zone where, without additional measures, an incident can have life-threatening consequences for people inside buildings [1]. There are three different focus areas, for toxic clouds, explosions (overpressure) and fire (heat radiation). Focus areas help policymakers to decide whether additional protective measures are needed.

At the moment, the boundary of the fire focus area is defined as the distance at which the heat flux can reach 10 kW/m^2. However, the effect of heat radiation is determined by (at least) two parameters: the heat flux and the duration. In a preliminary study, RIVM concluded that although the fire focus area would best be described with heat dose instead of heat flux only [2], there was insufficient information to recommend a particular dose relationship.

In 2023 the Ministry of Infrastructure and Water Management has asked the RIVM to do a follow-up study to develop a dose relationship for the calculation of the fire focus area. In this report the results of said follow-up study are presented.

1.1 Scope of this study

The goal of this study is to develop a better method to determine the boundary of fire focus areas. The study is limited to the heat radiation of accidental industrial fires. This report does not deal with in-building fires, spreading fire (direct flame contact) or the effects of smoke.

1.2 Methodology

The following steps are done to develop a dose relationship for the calculation of the fire focus area:

1. Different mechanisms in which a heat flux may endanger people inside buildings are reviewed. The results are described in Chapter 2.
2. As secondary fires are considered to be the primary danger to people inside buildings, a literature search is done to the effect of external heat radiation on materials found in and near buildings (private homes, office buildings, sheds, caravans, tents, …) and the initiation of secondary fires. The results of the literature study are described in Chapter 3.
3. Based on the literature search, a dose relationship for the initiation of secondary fires is developed. (Chapter 4).
4. The dose relationship is calibrated with four incidents of high pressure natural gas pipelines (Chapter 5).

[1] In Dutch: *plaatsgebonden risico* and *groepsrisico*

5. The differences between the fire focus area based on a heat flux (10 kW/m^2) and a fire focus area based on a radiation dose for various scenarios are shown in Chapter 6.
6. Finally, the conclusions and recommendations are described in Chapter 7.

1.3 Advisory committee

During the study, an advisory committee of experts was involved to advise on the research to be done and to comment draft reports. The members of the advisory committee were:

- Marc Dröge, Gasunie
- Joost de Klerk, DCMR Environmental Protection Agency (DCMR Milieudienst Rijnmond)
- Stefan Musch, Omgevingsdienst Noordzeekanaalgebied (ODNZKG)
- Bruno Reiners, Government of Flanders, Department of Environment & Spatial Development
- Mark Schaerlaekens, Government of Flanders, Department of Environment & Spatial Development
- Margreet Spoelstra, Netherlands Institute for Public Safety (NIPV)
- Maarten Worp, Veiligheidsregio Rotterdam Rijnmond (VR-RR)

In addition to the advisory committee, Ruud van Liempd and Johan van der Graaf (both NIPV) were consulted as experts for sources of information. They provided input about how a heat flux may endanger people inside buildings and the initiation of secondary fires.

The authors thank the members of the advisory committee and the experts of the NIPV for their valuable contributions.

1.4 Terminology

In this report, the heat radiation of fires is described. In a fire **energy** (J, Joule) is released. The **power** of a fire is measured in energy per second (J/s or W, Watt). As the radiation travels away from the fire it will spread in two dimensions and the power per square meter will drop. Power per square meter is called **radiation flux** or **heat flux** (W/m^2, or in practice kW/m^2). The **radiation dose** is the exposure to a heat flux for a period of time. The unit of the radiation dose depends on the way it is calculated. In this report t is used for **time**, and T for **temperature**. All units are metric.

2 Danger to people inside buildings

An incident with flammable substances results, after ignition, in a fire, such as a flash fire, pool fire, jet fire or fireball. The resulting heat radiation may endanger people.

Direct exposure of people to high levels of heat radiation may result in second- or third-degree burns which may lead to death [3]. When people are in buildings they are not directly exposed to heat radiation. Although windows do not block heat radiation entirely we can assume that a person inside a building can find protection against direct exposure.

Even if direct exposure to heat radiation is avoided, heat radiation may still have life-threatening consequences for people in buildings through the following phenomena:

- the collapse of the building;
- too high temperature in the building;
- secondary fires of building materials.

2.1 Collapse of the building

Intense heat radiation weakens steel constructions and may result in the collapse of buildings. However, this phenomena requires high levels of heat radiation, in the order of 100 kW/m^2 or more for at least half an hour [4]. As will become clear in this report, the threshold for the initiation of secondary fires is lower [5, 6]. For brick and concrete buildings this is even less of an issue. Hence, the collapse of buildings is not used as criterion for the boundary of the fire focus area.

2.2 Too high temperature in building

Intense heat radiation will increase the temperature in a building. If the temperature becomes too high, people suffer death due to heat stroke, skin burns or respiratory tract burns. It is assumed that during the type of incidents for which the focus areas are intended fatalities will not occur below 60°C and may occur above this threshold [7]. For very long exposures hyperthermia may occur at lower temperatures. An example is the increased death rate among the elderly during very hot summers. High humidity will also increase the death rate (and lower the temperature at which people die). In the case of heating due to a fire the relative humidity will however drop, making this less of an issue. Nevertheless, it is important to note that firefighting efforts, such as water-based suppression techniques, may rapidly increase the indoor humidity in certain circumstances. The increase in humidity could exacerbate risks for those exposed, and as such, specific conditions should always be evaluated to avoid over-reliance on general assumptions of safety.

The heat radiation increases the air temperature inside the building indirectly. The building absorbs the heat radiation and warms up. This in turn increases the air temperature inside the building.

A simple calculation shows that a heat flux of 10 kW/m^2 on a brick wall with heat capacity 1.5 10^6 J/m^3.K and a thickness of 0.2 m leads to a 30°C temperature rise of the wall after 900 s. This is a very conservative approach by assuming that all radiation is absorbed and all heat loss terms due to conduction and convection are ignored. Furthermore, the temperature rise inside the building is hampered by unexposed walls. A heat flux of 10 kW/m^2 during 900 s is comparable to the threshold for the initiation of secondary fires as derived in Chapter 4. Given the very conservative approach, it is concluded that secondary fires initiate earlier during a fire than that the indoor temperature rises to dangerous levels. Therefore the temperature inside buildings is not used as criterion for the boundary of the fire focus area.

At high temperatures materials will decompose (pyrolysis), potentially releasing toxic gases. In Section 3.1 it is explained that literature data for piloted ignition is used. This means pyrolysis gases will combust immediately. The toxic effects will therefore not be considered.

2.3 Initiation of secondary fires

If a combustible material is exposed to heat radiation, it may catch fire if the combination of duration and intensity of the radiation is large enough. If materials near or in buildings catch fire, people in buildings may suffer life-threatening consequences. The radiation dose required for secondary fires is lower than the dose required for lethal temperatures in the building or required for the collapse of the building.

It is therefore proposed to use the initiation of secondary fires as boundary of the fire focus area [2]. The dose required for materials to catch fire is studied in the next chapter.

3 Literature study

A literature study was done to find the relation between heat radiation and time to ignition. This included papers describing the theory and models used to describe this relation, as well as experimental results. As will be described in the next section only data from piloted ignition experiments were used. A report by HSE [8] already contained a large amount of experimental data up to 2003 that has been used. Because of this, the search in our study was limited to papers published starting in 2000. A full list of search terms can be found in Chapter 8.

This chapter will first discuss what contributes to the ignition of materials. Then an empirical relationship between heat flux and time to ignition is discussed. In Section 3.3 the collected experimental data is presented and discussed. Section 3.4 discusses the findings of this chapter. This chapter is accompanied by the appendix in Chapter 8, where some additional information can be found.

3.1 The ignition of materials

A fire can heat materials in three ways: by conduction, by convection, and by radiation. Of these three, radiation will have effects at the largest distances.

The ignition of materials due to radiation happens in a three-phase process [9]:

1. the temperature of the material rises;
2. the material starts to pyrolyze (thermally decompose) [9-11];
3. the pyrolysis gases ignite.

A lot of research has been done on the ignition properties of materials, especially on predicting their behaviour when exposed to heat. Experiments are done where samples are irradiated with various heat flux levels. This is done using a cone calorimetry setup. In *autoignition* experiments the heat radiation is responsible for the ignition of the pyrolysis gases, in *piloted ignition* experiments a pilot flame or spark plug is used for ignition. In autoignition experiments materials take a longer time to ignite compared to piloted ignition experiments.

In this report the data from piloted ignition experiments is used. This is a more conservative approach as it takes the presence of an ignition source into account. For example dry leaves on a windowsill can ignite much faster than the windowsill itself, thereby becoming an ignition source for the windowsill. Glowing or burning material spread from the fire may become an ignition source. Both DNV [5] and HSE [8] also use piloted ignition for their dose relationship, for the same reasons.

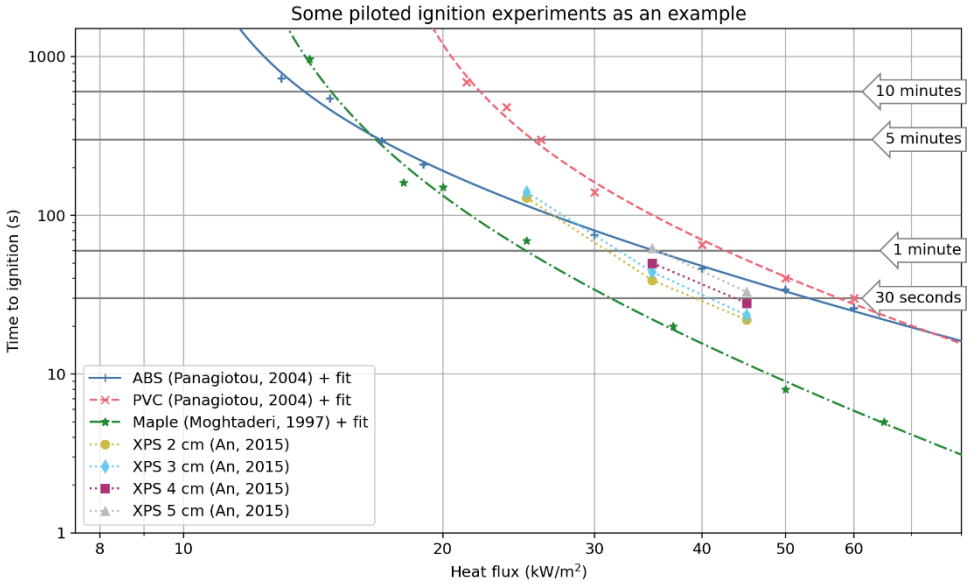

Figure 1 Some examples of the relation between heat flux and time to ignition, using piloted ignition experiments.[12-14] XPS is extruded polystyrene. Both axes are logarithmic.

Figure 1 shows the results of a few piloted ignition experiments. The materials in this plot are chosen as an illustration of the relation between heat flux and time to ignition. The materials are not representative of all data used in this study. The data for ABS[2], PVC, and maple show how the time to ignition changes for a large range of heat fluxes. At lower heat fluxes the time to ignition increases rapidly. Below a particular heat flux a material won't ignite at all, this is called the critical heat flux. The data for XPS[3] shows how the thickness influences the time to ignition.

Research shows that the temperature at which pyrolysis starts is more or less constant for a material [10, 15]. The speed at which the temperature of a material rises depends on the heat flux and the specific heat capacity[4] of the material, but also on how much radiation is absorbed and how much of the heat absorbed is removed by conduction and convection.

One variable, as was shown in Figure 1, is the thickness of the material. As the XPS sample becomes thicker, the time to ignition increases. At 25 kW/m^2 the thickest two sample didn't even ignite within the 600 second (10 minute) duration of the experiment. [13]

Another area of research is the effect of moisture content in the materials. Khan et al studied corrugated cardboard and found that samples with a higher moisture content took longer to ignite, although this only made a difference at higher heat fluxes. [16] Spearpoint et al showed that wood with a higher moisture content takes longer to ignite. Their explanation is that moisture influences the conduction of heat and

[2] Acrylonitrile butadiene styrene, for example known from Lego bricks and 3D printing
[3] Extruded polystyrene
[4] Specific heat capacity is the amount of energy needed to heat up 1 kg of material by 1°C.

the heat capacity of the material. [17] Safronova et al found that for plastics a higher moisture content resulted in a *shorter* time to ignition. Their explanation is that steam results in small bubbles in the plastic, making it easier to ignite. [18]

Spearpoint et al also showed that the orientation of wood – along or perpendicular to the grain – makes a difference. [17]

The goal of the papers studying all these different variations is to build theoretical models to explain and predict the ignition behaviour of materials. To do this, many material properties need to be known. To determine the dose needed to ignite materials a simpler empirical model can be used, as will be described in the next section. These models can describe the complexities of the results without explaining them. This dose relationship can then be used to determine the distance at which secondary fires can occur.

3.2 Dose relationship

In this section a phenomenological relationship between the heat flux R (kW/m^2) and exposure time t (s) is described. Materials will ignite if, after a certain time t_{ig}, they have reached the reference dose A. Reference dose A depends on the properties of the sample, as discussed in the previous section.

In practice, to fit the dose relationship with experimental data, two additional parameters are used. First is the critical heat flux C (kW/m^2) below which materials do not ignite. Only heat fluxes at or above the critical heat flux are included in the calculation. Second is a factor B (dimensionless) to scale the heat flux. This results in the following equation:

$$t_{ig} = \frac{A}{(R-C)^B} \qquad \text{3-1}$$

The unit of A is now $s \cdot \left(\frac{kW}{m^2}\right)^B$. Both B and C depend on the properties of the sample.

Equation 3-1 is also used for the dose relationship of Bilo et al [6], HSE [8], and DNV [5].[5] DNV [5] uses the parameters $A = 17500\ s \cdot \left(\frac{kW}{m^2}\right)^2$, $B = 2$, and $C = 12\ kW/m^2$.

Bilo et al found $A = 1288\ s \cdot (kW/m^2)^{1.5}$, $B = 1.5$ and $C = 14.7\ kW/m^2$. [6] In their 2006 review of ignition criteria HSE however uses a different critical heat flux of 12.6 kW/m^2, while leaving the other parameters equal.[8] In this report the dose relationship with $A = 1288\ s \cdot (kW/m^2)^{1.5}$, $B = 1.5$ and $C = 12.6\ kW/m^2$ is referred to as "HSE".

According to Silcock et al the value of B depends on whether a material is thermally thin or thick. For a thermally thick material the physical

[5] There are some minor differences, explained in Section 8.2. These differences are not relevant to the discussion.

thickness of the sample is not relevant, while for a thermally thin material it is. In experiments they find values between 1 and 2. [19]

Equation 3-1 can be used to relate heat flux to time to ignition for cases where the heat flux is constant. For experiments with transient heat fluxes the radiation has to be integrated over time.

$$\int (R(t) - C)^B dt = A \qquad 3\text{-}2$$

3.3 Literature data

The time to ignition for piloted ignition experiments with constant heat flux from 25 different papers were collected, giving over 600 datapoints. The results are shown in Figure 2. A detailed list with sources is given in Section 11.1, all data is listed in Section 11.2.

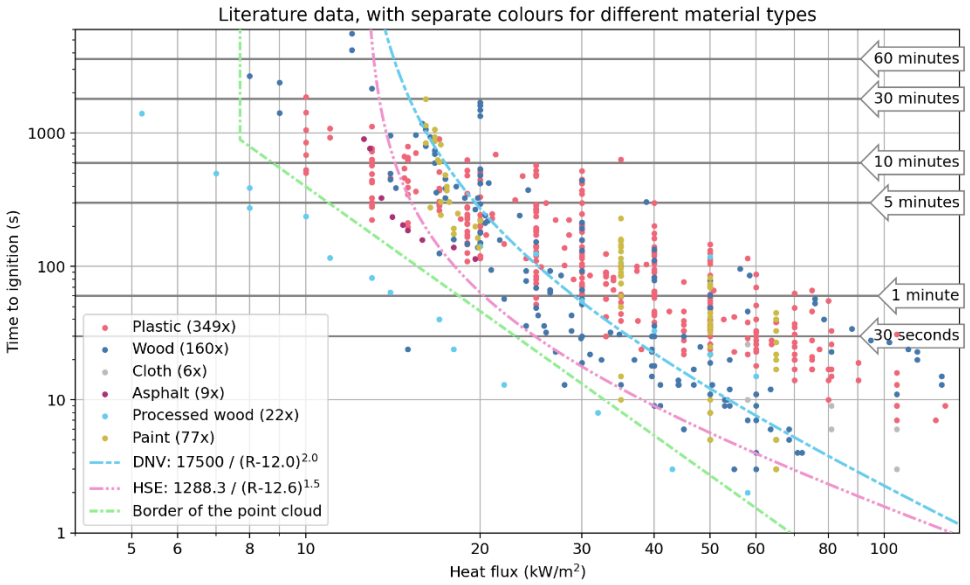

Figure 2 Log-log plot of the time to ignition for different materials. The dashed pink line and dotted blue line are the dose relationships according to DNV [5] and HSE [8], respectively. The dash-dotted green line is to guide the eye and is discussed in the text.

The heat flux is shown on the x-axis, the time to ignition on the y-axis. Every dot is a single data point from literature, and in effect shows the dose needed for that particular sample to ignite. The colours of the dots indicate the type of material used. The legend also shows the number of data points per material. The dose relationships for DNV and HSE are plotted as well. There are a few things to notice.

First is that there seems to be a point cloud that contains most datapoints. In the figure this is shown by the dashed green border. On the lower left side of this border is the data of processed wood ("fibre insulation board") which seems to be valid data [20]. There is also a single blue datapoint. This seems to be an outlier but is not identified as such in the paper [21]. In some analyses these datapoints are considered separately.

It is also noticeable that there is also a very limited amount of data available below 10 kW/m^2. The reason for this is unknown to us. We speculate that it was considered as not interesting because of the long time to ignition. Another reason may be limitations of the experimental setup.

Second is that the behaviour of Equation 3-1 can be seen from the dose relationships of DNV and HSE. Below the critical heat flux C (12.0 and 12.6 kW/m^2 respectively) the dose is not calculated. At the critical heat flux the time to ignition is infinite. As the heat flux increases, the time to ignition drops quickly. The time to ignition is listed in Table 1, for both the data collected in this study and the dose relationships by DNV and HSE.

Table 1 Overview of the time after which the first material will ignite. The left column shows this for the literature data, ignoring the data for processed wood and an outlier. The middle and right column show the time to ignition calculated using the DNV and HSE dose relationships.

kW/m^2	**Data**	**DNV**	**HSE**
10	8m 24s	-	-
13	3m 43s	4h 52m	1h 25m
15	3m 7s	32m	5m 47s
20	1m 49s	4m 33s	1m 4s
30	13s	54s	18s
40	9s	22s	9s
50	5s	12s	6s
60	3s	8s	4s

The dose relationships of both DNV and HSE do not seem conservative, judging by Figure 2 and Table 1. The DNV dose relationship predicts a longer time to ignition for all heat fluxes, and by a very large margin for 13 and 15 kW/m^2. The HSE dose relationship predicts a longer time to ignition for 13 kW/m^2 and comparable times to ignition for higher heat fluxes. In addition, 39% of the datapoints in the graph are below the curve of DNV, i.e. the materials will ignite faster than predicted by the dose relationship. In both cases the critical heat flux is too high. The data shows that materials can ignite well below 12 kW/m^2.

The third thing to notice in Figure 2 is a difference between wood and plastic. To make this more clear, Figure 3 shows the literature data of wood and plastic. It seems that below 20 kW/m^2 the first materials to ignite are plastics, while above 20 kW/m^2 this is wood.

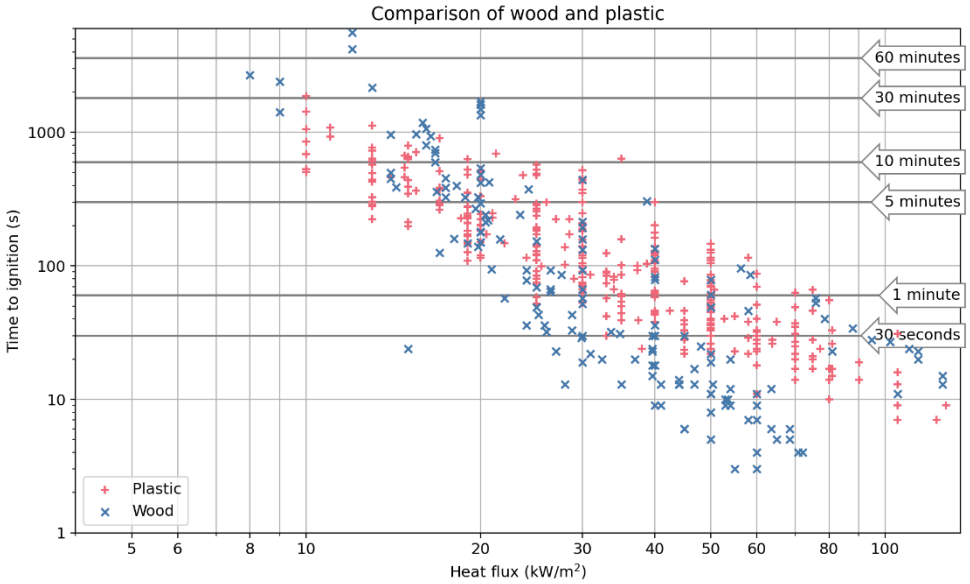

Figure 3 Log-log plot of the literature data on the time to ignition for wood and plastic.

The dose relationships of both DNV and HSE have been (partially) based on experimental data on the time to ignition for wood [5, 8]. This may explain why these dose relationships do not seem conservative. In the next section the differences in ignition behaviour between wood and plastics are studied further.

3.3.1 *Difference between wood and plastic*

To further study the difference between wood and plastic individual data sets were studied. A data set is a collection of measurements where all parameters stay the same, except for the heat flux.

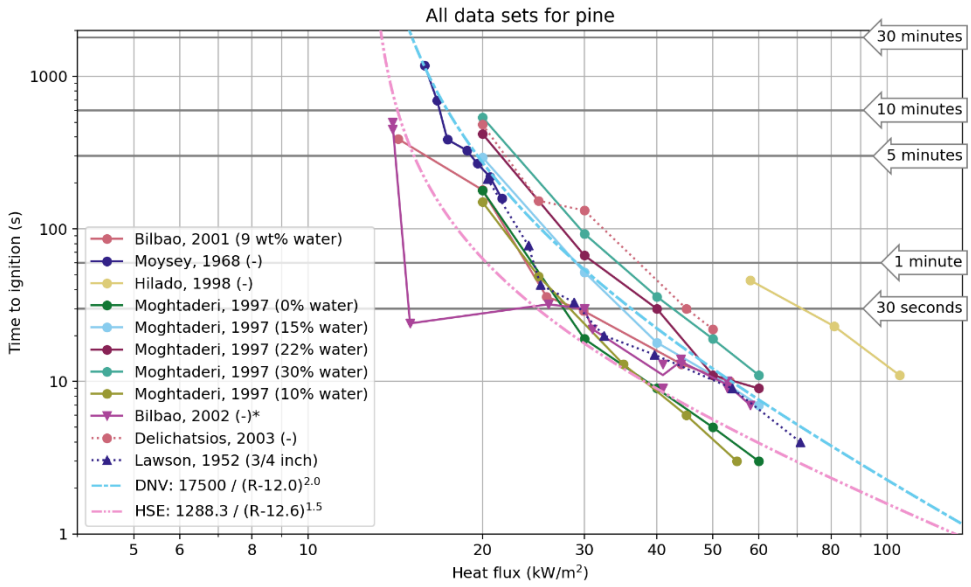

Figure 4 Data sets with pine wood. In some cases a single heat flux was measured multiple times, in this case the two results were averaged. This is indicated in the legend with an asterisk.

Figure 4 and Figure 5 show the individual data sets for pine wood and PMMA (Perspex). Additional plots with data sets are included in Section 8.3.

In both figures there is a clear spread between the data sets. The data sets for pine more or less follow the dose relationship of DNV and HSE and a critical heat flux between 10 and 15 kW/m^2 seems realistic. The data sets for PMMA are not as steep as those for pine and there is no sign of it sloping upwards. It is clear that the critical heat flux has to be below 10 kW/m^2.

No measurement data of PMMA at fluxes below 10 kW/m^2 have been found. Silcock et al measured the time to ignition for PMMA and they extrapolated the results to find a critical heat flux of 9.0 kW/m^2 for extruded PMMA and 5.0 kW/m^2 for cast PMMA. This was determined based on data measured between 10 and 50 kW/m^2.[22] An extrapolation by Rhodes et al of their data gives a critical heat flux of 4 kW/m^2 [23], this was done using data between 15 and 40 kW/m^2.

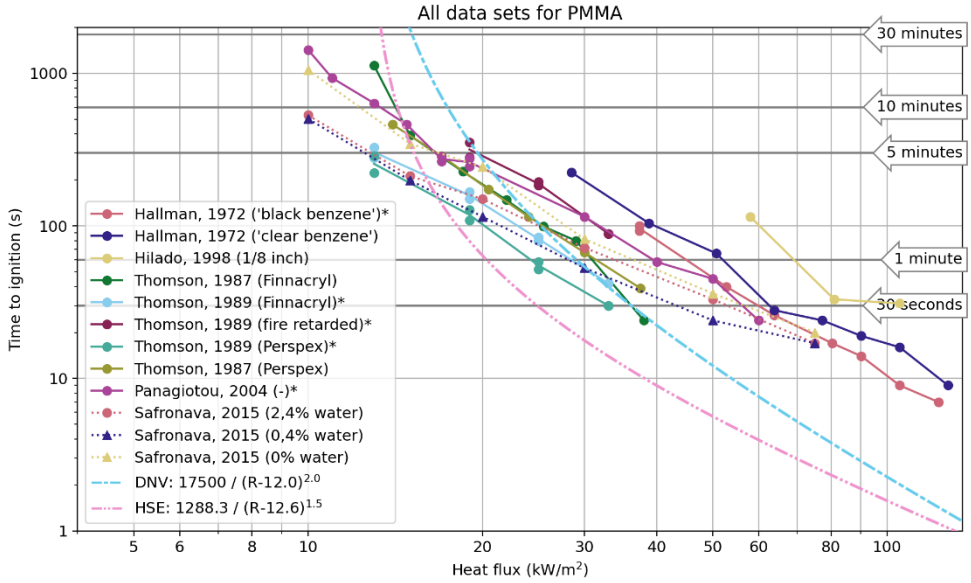

Figure 5 Data sets with PMMA. An asterisk indicates when two measurements at the same heat flux were averaged.

3.3.2 Relevancy of materials

A list of all materials is included in Chapter 11. The materials can be found in built-up areas. We recognize four limitations in the data available.

First is that most materials are untreated. Coatings, like paint, introduce a number of extra variables: the coating used, the thickness of the coating, the substrate on which it is used. Staggs et al writes that for up to two layers of paint the time to ignition will increase, but that more layers of paint will reduce the time to ignition by up to a factor 7 compared to the untreated material. [24] Moysey et al writes that there is almost no difference between painted and unpainted cedar wood.

They think this is because the paint scorched and broke down at relatively low heat fluxes. [25]

Second is that all materials are, presumably, close to new. It is unclear how materials behave after 10, 20 or more years in use. As in the previous case including aging would introduce more variables.

Third is that reed, used for thatched roofs, is not included. Fire safety literature for thatched roofs focusses on the danger of aerial embers, not radiation.

Finally, as discussed above, there was a lack of data below 10 kW/m^2. It was considered outside the scope of this study to do experiments at lower radiation levels and no measurements were done.

Despite these limitations it was concluded that the data set covered a wide enough range of materials to be sufficient for determining a dose relationship.

3.4 Discussion and conclusions

Data on the time to ignition for different heat fluxes, using piloted ignition, was collected from literature. The materials cover common materials found in and around buildings. Treatment of materials with coatings and aging of materials is not taken into account. We recognize this limitation but concluded the data set is still sufficient.

The result is a point cloud that, aside from one measurement and an outlier, seems to have a clear edge. This suggests it should be possible to derive a dose relationship for secondary fires due to heat radiation. The data shows us a few things about how such a relationship could look like.

Literature agrees that materials like wood and plastic, as well as other materials that can be found in and around built-up areas, have a critical heat flux, below which an individual material will not ignite due to heat radiation. This critical heat flux differs per material. From the data it is clear that for some materials the critical heat flux is below 10 kW/m^2, but a lack of data makes it difficult to be precise. Given the data found in this literature study the dose relationships used by DNV and HSE are not conservative approaches for determining when secondary fires may start. With 12.0 and 12.6 kW/m^2 their choice for the critical heat flux seems reasonable for wood, but too high for other materials like plastics.

4 Derivation of a dose relationship

The literature study returned a lot of data on the relation between heat flux and time to ignition. A plot of the data shows a point cloud that, for the most part, can be surrounded by the green border in Figure 2. This green border can however not be used for a dose relationship. In this chapter a dose relationship will be derived.

In short, it was decided to use Equation 3-1 as the dose relationship (Section 4.1). Factor B was derived by fitting all data to the dose relationship with $C = 0\ kW/m^2$ (Section 4.2.1). Then the reference dose A was calculated for three different critical heat fluxes and five different percentile values of the number of points below the curve (Sections 4.2.2 and 4.2.3). The results were evaluated against the literature data (Sections 4.2 and 4.3, and in more detail in Appendix 9.2), resulting in a range of possible values for A and C. In the next chapter the dose relationship is calibrated against four accidents with pipelines (Sections 5.1 - 5.3). In addition, a sensitivity analysis of B was done (Section 5.4) and the change of the distance to the reference dose in time was performed (Section 5.5).

4.1 Guiding principles

4.1.1 Using all data

Both DNV [5] and HSE [8] derived their dose relationship using one or a few materials they deemed representative. The literature study however showed that materials behave very differently and it was decided to use all collected data instead. As discussed in the literature study, the experimental data seems representative of materials found in and around buildings. This means that for the derivation of the dose relationship all literature data was used. In some cases the results were also calculated without the dataset for processed wood and the outlier, to check if these data points distort the outcome. If this is the case it is explicitly mentioned.

4.1.2 Characteristics of the dose relationship

The dose relationship should take the following into account:

1. a slope to represent the inverse relationship between heat flux and the time to ignition;
2. a critical heat flux below which materials do not ignite;
3. a reference dose for when materials catch fire.

A relationship where the time to ignition changes continuous instead of in steps was preferred.

The dose relationship of Equation 3-2 (reproduced below for readability) includes the required components: a critical heat flux C (kW/m^2), a factor to adjust the slope B (unitless), and a reference dose A ($s \cdot (kW/m^2)^B$).

$$\int (R(t) - C)^B dt = A \qquad 4\text{-}1$$

This relation is normally used to phenomenologically describe the relationship between heat flux and time to ignition for *individual* materials. It does however fit all the characteristics needed.

4.1.3 *Behaviour of the dose relationship*

This section will explore how the dose relation changes when the parameters are changed. Figure 6 shows how changing parameter A or B or C changes the dose relationship.

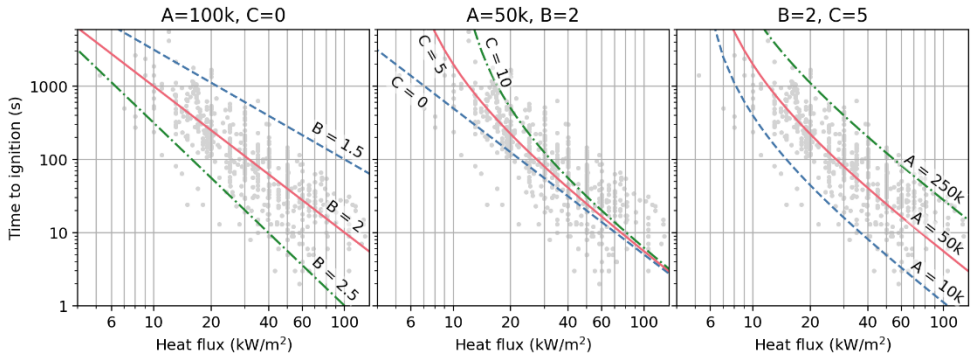

Figure 6 Visualization of the parameters. Because of space constraints, "k" is used as shorthand for thousand and units are not shown.

As long as the denominator $(R - C)$ is not close to zero, factor B determines the slope of the curve, as is shown in the left panel of Figure 6. B is dimensionless. For $B = 1$ and $C = 0\ kW/m^2$ there is a linear relationship between the heat flux R and time to ignition t_{ig}, i.e. the time to ignition will be twice as long if the heat flux is halved. When $B = 2$ and $C = 0\ kW/m^2$ the time to ignition will be four times longer if the heat flux is halved.

As the heat flux approaches critical heat flux C (in kW/m^2) the time to ignition will start to increase rapidly, as is shown in the middle panel. For $C = 5$ and $10\ kW/m^2$ this is visible, but for $C = 0\ kW/m^2$ this occurs left of the plot. The critical heat flux reflects that materials will not ignite below a certain heat flux.

Finally, the right panel shows the effect of changing the reference dose A. Its unit depends on B: $s \cdot \left(\frac{kW}{m^2}\right)^B$. A higher reference dose means the time to ignition will increase and more datapoints will be below the curve, i.e. they will ignite earlier than the dose relationship calculates. In this plot for $A = 10{,}000\ s \cdot \left(\frac{kW}{m^2}\right)^2$ the percentile is about 3%, while for $A = 250{,}000\ s \cdot \left(\frac{kW}{m^2}\right)^2$ it is about 97%.

4.1.4 *Piloted ignition versus auto ignition*

As discussed in Section 3.1 piloted ignition is a conservative choice in comparison with auto ignition. We found one paper where a relation for both piloted and auto ignition were derived, by Bilo et al.[6] They used American whitewood to derive a dose relationship for both piloted and auto ignition. They found $A = 1288\ s \cdot (kW/m^2)^{1.5}$, $B = 1.5$ and $C = 14.7\ kW/m^2$ for piloted ignition and $A = 603\ s \cdot (kW/m^2)^{1.25}$, $B = 1.25$ and $C = 25.6\ kW/m^2$ for auto ignition.

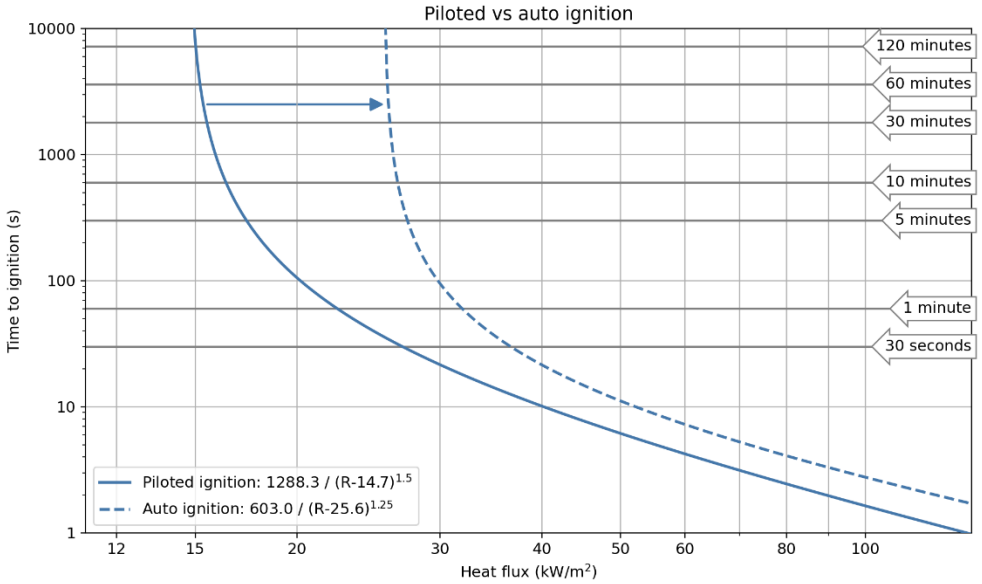

Figure 7 Piloted and auto ignition for Bilo et al.

Figure 7 shows the dose relationships for Bilo et al for both piloted and auto-ignition. The critical heat flux is clearly higher and at higher heat fluxes there remains a difference in the time to ignition.

4.2 Method of derivation

The previous section showed how the dose relationship changes when the individual parameters are changed. It was decided to determine the value of factor B first as the point cloud has a definite slope. The literature study didn't give a clear value for the critical heat flux C. The reference dose A can change significantly if B and C change. It was decided to instead take the value for A when a given number of data points were below the curve (i.e. ignite earlier than calculated by the dose relationship).

The results of the dose relationship with a range of values for C and percentile values were evaluated against the literature data. Section 4.3 summarizes the results, the appendix in Chapter 9 discusses the evaluation and the results in more details.

The results were then compared with a number of actual pipeline fires.

4.2.1 Derivation of factor B

Factor B was found by fitting[6] all data to

$$t_{ig} = \frac{A}{R^B} \qquad 4\text{-}2$$

I.e. the dose relationship with $C = 0\ kW/m^2$. This fit results in $B = 2.0$.[7] This corresponds to a thermally thick material, according to Silcock et al. [19]

[6] Using the scipy.optimize.curve_fit function
[7] To be precise: $B = 1.99818898$

This way of fitting B depends on the available data. If for example the data from processed wood and the outlier are left out, the fit will give $B = 2.1$. The difference between B with and without these data is small and shows the sensitivity is limited.

In the sensitivity analysis in Section 5.4 $B = 1.5$ and 2.5 are also used, since the former is the factor B used by HSE.

4.2.2 *Selection of critical heat fluxes C used in the analysis*

First, the range for C was determined.

In countries near the equator the heat radiation from the sun can reach 1 kW/m^2 and materials don't ignite there, even after long exposure to the sun. The critical heat flux should therefore be above 1 kW/m^2.

From the literature study it emerged that even though there is very little data below 10 kW/m^2, the critical heat flux should be below that. This choice may appear conservative. This is lower than used by DNV [5], HSE [8], and a paper by Bilo and Kinsman [6]. In all these cases the critical heat flux was based on the ignition of wood. In our literature study it emerged that plastics have a much lower critical heat flux.

It was decided to choose $C = 3$, 5, and $8\ kW/m^2$.

4.2.3 *Selection of percentile values to find reference dose A*

Given the values for B and C, the value of A is determined by choosing the percentile value, i.e. the percentage of points that are below the curve. When a data point is below the curve it means the time to ignition is shorter than the dose relationship predicts. Unless the dose relationship is extremely conservative some data points will be below the curve. A higher percentile value will result in a higher reference dose.

The selection of percentile values used in an analysis depends on the data set available. The data points for processed wood and the outlier constitute about 2.5 percent of the data. A percentile value close to that would quickly result in a very conservative dose relationship. On the other hand, when a percentile value of 40 or 50 percent has to be used it raises questions about if this dataset can be used for this purpose.

In their report DNV uses parameters $A = 17500\ s \cdot \left(\frac{kW}{m^2}\right)^2$, $B = 2$ en $C = 12\ kW/m^2$. With our dataset this corresponds to a percentile value of 39%.

For this study we choose 10, 20, 30, 40, and 50 percent.

4.2.4 *Data processing*

All data was processed in Python 3.11.4. Numpy 1.25.1 [26] and Scipy 1.11.1 [27] were used for calculations, Pandas 2.1.0 was used for data management, and Matplotlib 3.7.2 was used to produce the plots.

The reference dose was found by calculating the dose for all datapoints using Equation 4-1, with the heat flux R_i and the time to ignition t_i of the

datapoints and the given values for B and C. This resulted in dose A_i for all datapoints.

Next, an initial value of the reference dose was selected. The fraction of the number of points with a dose A_i less than the initial value was calculated and compared to the percentile value chosen. If the fraction was less than the percentile value, the value of the refence dose was raised with 10 and the process was repeated. Finally, the value of the reference dose where the fraction was closest to the percentile value was chosen. Due to the step size of 10, there are minor differences in the actual fraction of points below the curve compared to the percentile value.

4.3 Summary of the results from comparison with the literature data

Using the parameters described above the dose relationships have been calculated. This section summarizes the results, the full results and a more detailed discussion is included in Section 9.2.

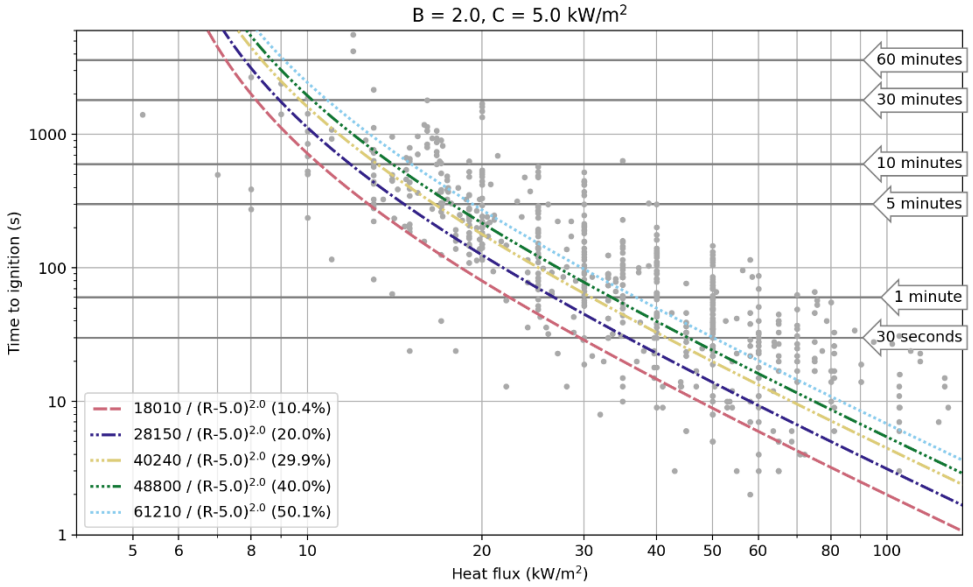

Figure 8 Results for B = 2 and C = 5 kW/m², for different percentile values. The number between brackets is the actual percentage of points below the curve.

Figure 8 shows how the dose relationship changes for a fixed critical heat flux and varying percentile values, for a single case. A higher percentile value will result in a higher reference dose and a longer time to ignition.

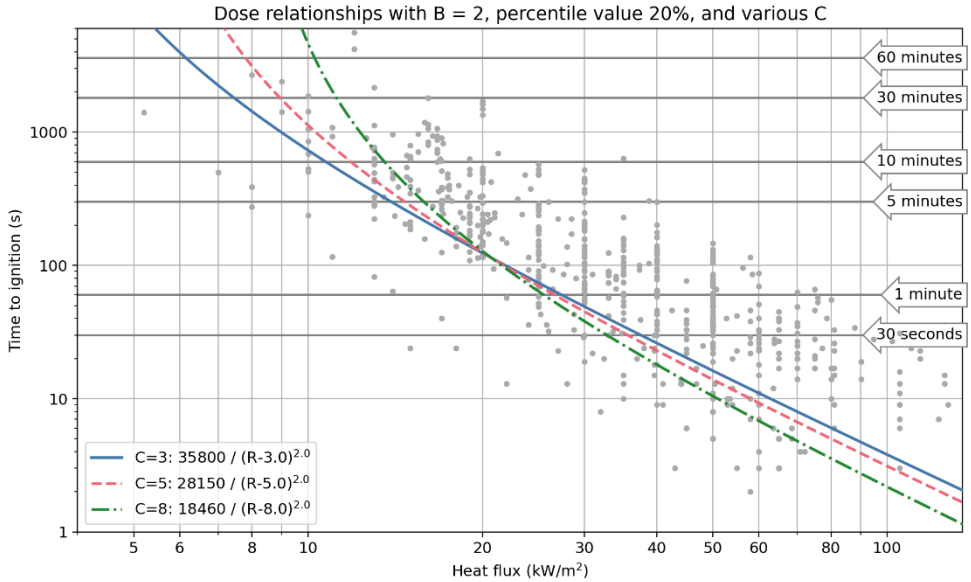

Figure 9 Results for B = 2 and a percentile value of 20%, for different critical heat fluxes.

While Figure 8 shows the results for different percentile values, Figure 9 shows it the other way around: a fixed percentile value and different critical heat fluxes. The reference dose can not be compared directly because the denominator is different. For higher critical heat fluxes the time to ignition is longer for low heat fluxes and shorter for high heat fluxes. The reason is that for higher critical heat fluxes there are more points below the curve at low heat fluxes and, because the total number has to remain the same, fewer points can be below the curve at higher heat fluxes.

Something to note in Figure 9 is how the curve behaves at and below $R = 12\ kW/m^2$. For C = 8 kW/m^2 all datapoints are below the curve. Our conclusion is that C = 8 kW/m^2, with the parameters chosen in this graph, does not describe the data well enough at lower heat fluxes.

4.4 Discussion and conclusion

This chapter discussed how the dose relationship behaves in general, how the value for B was determined, and why the choices for particular values of C and the percentile value were made. Using these parameters, an evaluation was made of the literature data. This resulted in valuable insight into the behaviour of the dose relationship, and excluded certain combinations of parameters. However, it didn't result in a single parameter set that could be used. In the next chapter four accidents with high pressure natural gas pipelines are used to calibrate the dose relationship.

5 Calibrating the dose relationship with data from previous accidents

In the last chapter an analysis was done of the dose relationship in relationship with the literature data on piloted ignition. Factor B was derived to be 2. For the critical heat flux C and the percentile value (as a way to determine the reference dose A) a range of possible values were used. In this chapter the dose relationship will be calibrated using four real-world accidents with high pressure natural gas pipelines.

In Section 5.1 the selection of accidents is discussed. An approximation of the distances where secondary fires occurred (for convenience shortened to "damage distance") was made. Section 5.2 describes how the fire was modelled in Safeti-NL[8]. Using the output of Safeti-NL the dose was calculated for a range of parameters for the percentile value and critical heat flux. In Section 5.3 the results are compared with the damage distance. The goal is to find distances that are slightly conservative compared to the distances of these fires. In Section 5.4 a sensitivity analysis is done for parameter B. Section 5.5 shows how the dose changes as a function of time. Finally, Section 5.6 has a discussion and conclusion.

5.1 Accident selection

Accidents were selected based on three criteria:

1. There has to be enough data to model the fire with reasonable accuracy. This is primarily the diameter of the pipeline, the pressure at the time of the accident, and the weather conditions.
2. There has to be enough information to estimate the damage distance.
3. There should be a relationship between the fire and the damage.

The third criterium excludes accidents where there was also a cloud fire (which would be a second source of damage). It also excludes fires where firefighters intervened to protect buildings at a large scale (which would cause the damage to be underestimated). In practice this limited the search to jet fires and specifically pipeline fires. In the selected fires the fire brigades had limited means to intervene, given the scale of the incident. Pool fires burn for a long time, but the intervention of the fire brigades makes it difficult to judge the duration and level of exposure.

The databases from the NTSB (US) and TSB (Canada) were searched for accident reports. Both databases contain in-depth reports with extensive factual information about the conditions at the time of the rupture. The description of the damage is not as extensive, especially when the incident occurred in remote areas. Three incidents in the US occurred in built-up areas and the damage was described. In Canada most incidents occurred in remote areas.

[8] Safeti-NL is a version of DNV Safeti used to calculate QRA's in the Netherlands. The consequence calculations are the same in both versions, but most options are fixed to the values prescribed in Dutch regulations.

The pipeline accidents in Ghislenghien (Belgium) and Ludwigshafen (Germany) have also been considered. Both countries do not have (had) an equivalent of the NTSB or TSB and no public reports were found. Via private communication some information was received about the accident in Ludwigshafen. Extensive photo archives on news websites also gave a good impression of the damage. This was however not the case for the accident in Ghislenghien. It was decided to include the accident in Ludwigshafen and not the accident in Ghislenghien based on criterium 2.

5.1.1 *September 9th, 2010: San Bruno, California, US*

A 743 mm pipeline carrying natural gas at 26.6 barg, ruptured in a suburb of San Bruno, California (near San Francisco) on September 9th, 2010. Eight people were killed and numerous were wounded. 38 houses were destroyed, 17 houses received damage where repairs had to be made before they could be occupied, and 53 houses received light damage.

The map by the NTSB (Figure 10) gives information about the damage. The wind was from the west-north-west, and this corresponds to most of the damage being on the east side. A house at 150 meter north of the fire was destroyed. On the west side a house was destroyed at 177 meter. The extend of the damage of the houses in the north-west corner, at 200 meter from the fire, is unknown and it can not be determined if this was an unsafe distance. Considering this the damage distance was estimated to be between 150 and 180 meter.

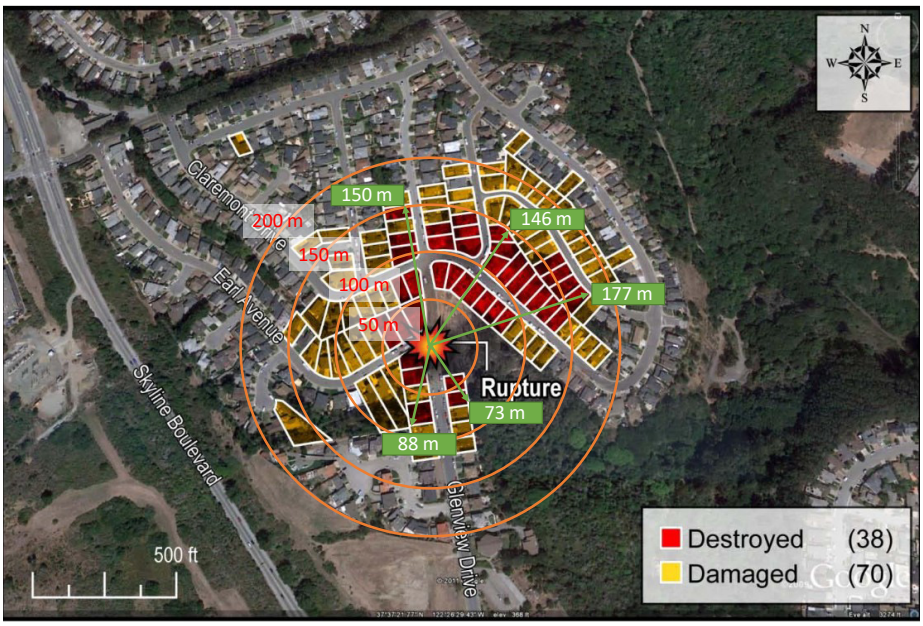

Figure 10 A map showing the damage from the pipeline fire. Source: NTSB [28] with annotations by the authors of this report.

5.1.2 *December 11th, 2012: Sissonville West Virginia, US*

A 494 mm pipeline carrying natural gas at 64 barg ruptured in Sissonville, West Virginia, on December 11th, 2012. There were no fatalities or wounded, but three houses burned down and a few more were damaged.

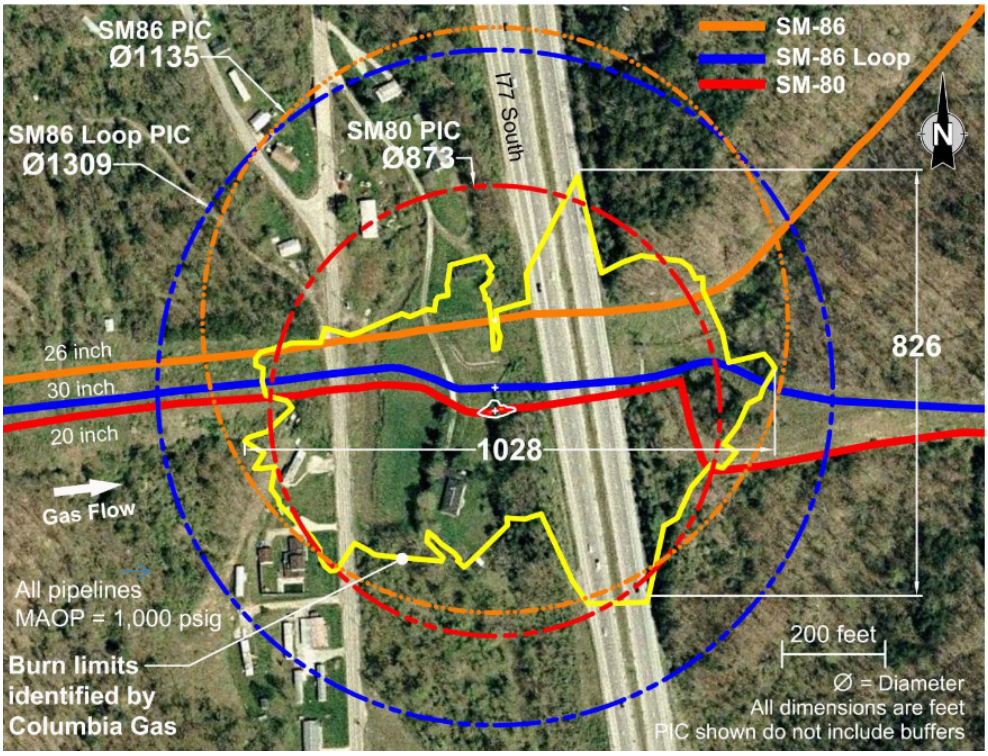

Figure 11 An overview of the damage of the Sissonville pipeline rupture. There were three pipelines (SM-86, SM-86 loop, and SM-80). SM-80 (red) ruptured. The circles are the calculated danger zones determined by the owner of the pipeline, Columbia Gas. The yellow line shows the observed burn limits. Source: NTSB [29]

Figure 11 shows the extent of the fire damage. The house on the west side, just inside the burn limits, burned down. The house just south of that did not. The estimation of the damage distance was taken to be halve 826 and 1028 feet: 125 to 165 meter.

5.1.3 *October 13th, 2014: Ludwigshafen, Germany*

A 400 mm pipeline carrying natural gas was damaged in the German city of Ludwigshafen on October 13th, 2014. One person was killed.

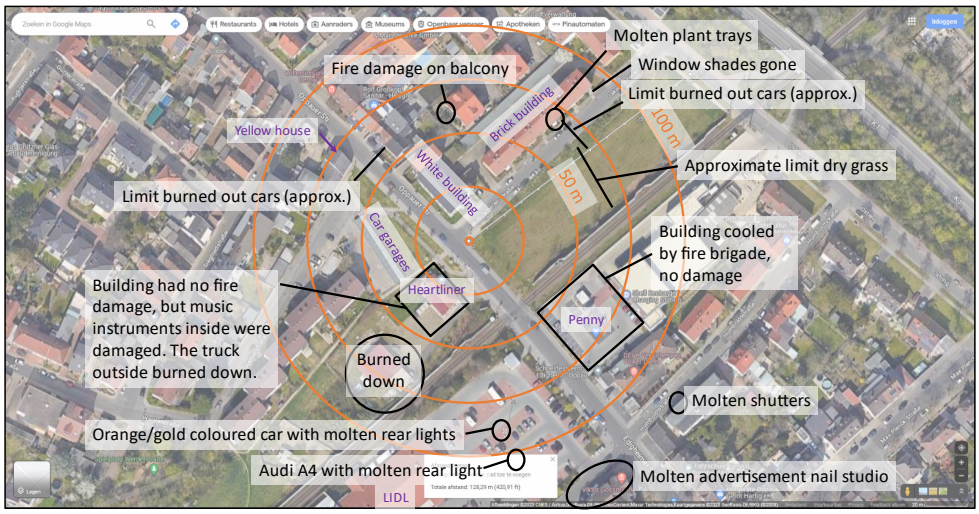

Figure 12 damage due to the fire in Ludwigshafen. Source: Google Maps, with annotations by the authors.

There was no official accident report, the data for Safeti-NL was obtained from private communication with Marc Dröge (Gasunie). The damage has been determined based on numerous photos in media [30-33]. This was the basis for the map in Figure 12. Between 60 and 75 meter cars caught fire. The concrete building labelled Heartliner did not show fire damage, but the shed southwest of it did burn down. At a distance of 90 meter sunshades were gone (possibly burned), and at approximately 125 meter a plastic advertisement melted down. On the basis of this information the damage distance was estimated to be between 60 and 75 meter.

5.1.4 *August 1st, 2019: Danville, Kentucky, US*

A 743 mm pipeline carrying natural gas at 63.8 barg ruptured in Danville, Kentucky. One person was killed and six injured. Five houses were destroyed and thirteen damaged.

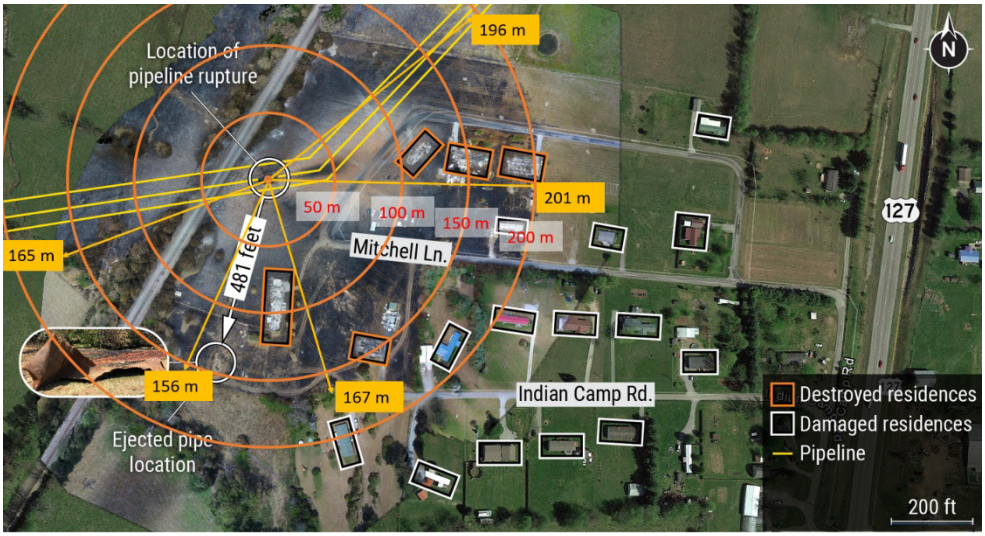

Figure 13 Damage after the pipeline rupture in Danville. Source: NTSB [34] with annotations by the authors.

On the east side a house was destroyed at 200 meter. On the south-south-west side a house was destroyed at 160 meter. These distances were taken as the upper and lower estimate of the damage distance.

5.2 Calculations

The calculations were done in Safeti-NL 8.8 using the long pipeline model, using methane.[9] Safeti-NL 8.8 does not give the proposed heat radiation dose as output. Therefore, the following steps were done:

- The release was averaged for the time steps listed in Table 2. The calculations are done for 1800 seconds because in the Netherlands scenarios in QRAs are limited to 1800 seconds.[10]
- For each time step the resulting heat flux as a function of distance was exported. The distances were interpolated to 1 meter to create a constant grid.
- At each distance, the dose was calculated by adding up the contributions of each time step.

Table 2 time steps for which the release was calculated

Time steps (seconds)
0-20
20-60
60-200
200-400
400-600
600-800
800-1000
1000-1400
1400-1800

5.3 Results of calibration

Using the heat flux calculated by Safeti-NL the dose was calculated for a range of parameters of critical heat flux C (kW/m^2) and several percentile values (the percentage of data points below the curve, see Section 4.2.3). The dose was also calculated using the dose relationships by HSE and DNV. Finally the distance to the 10 kW/m^2 boundary was determined. The results are summarized in Table 3. Colours were used to show how the result of the dose calculation compared to the lower and upper estimate of the damage distance.

[9] DNV.com - When trust matters - DNV
[10] A discussion about this limit is beyond the scope of this report.

Table 3 Distances (in meter) to lower and upper estimate of the damage distance, the distance to the 10 kW/m2 boundary, the reference dose using the HSE and DNV dose relationships, and the reference dose parameters critical heat flux (C, kW/m2) and percentile values, for B=2. The values for C = 3, C = 5 at the 10% en 20% percentiles have been highlighted as the best fitting values.

	San Bruno			**Sissonville**		
Damage distance (low)	150			130		
Damage distance (high)	180			165		
Distance to 10 kW/m2	321			292		
Distance HSE	211[c]			174[c]		
Distance DNV	184[c]			144[b]		
	C = 3	C = 5	C = 8	C = 3	C = 5	C = 8
10%	227[c]	219[c]	215[c]	199[c]	187[c]	180[c]
20%	209[c]	204[c]	200[c]	182[c]	173[c]	165[b]
30%	196[c]	193[c]	192[c]	170[c]	162[b]	157[b]
40%	190[c]	187[c]	184[c]	164[b]	156[b]	149[b]
50%	182[c]	180[b]	176[b]	157[b]	150[b]	142[b]

	Ludwigshafen			**Danville**		
Damage distance (low)	60			160		
Damage distance (high)	75			200		
Distance to 10 kW/m2	170			419		
Distance HSE	63[b]			184[b]		
Distance DNV	46[a]			134[a]		
	C = 3	C = 5	C = 8	C = 3	C = 5	C = 8
10%	116[c]	97[c]	77[c]	256[c]	225[c]	201[c]
20%	103[c]	88[c]	70[b]	224[c]	202[c]	176[b]
30%	94[c]	81[c]	65[b]	200[b]	183[b]	163[b]
40%	89[c]	76[c]	61[b]	189[b]	172[b]	151[a]
50%	82[c]	71[b]	56[a]	175[b]	160[b]	139[a]

[a] Shorter than the lower estimate of the damage distance
[b] Between the lower and higher estimate of the damage distance
[c] Longer than the higher estimate of the damage distance

In all four cases the distance to the 10 kW/m^2 boundary is much larger than the upper estimate of the damage distances observed in these accidents.

Using the dose relationship of HSE the distance to the reference dose is on the short side, but not a major underestimation. Using the dose relationship of DNV the distance is severely underestimated in two of the four cases.

The results show that a 10% percentile value always overestimates the damage distance. Percentile values of 40 and 50% regularly underestimate the damage distance. The same occurs for $C = 8\ kW/m^2$. The parameters for $C = 3$ or $5\ kW/m^2$ and 20 or 30% give the best fit (indicated by a box in the table). Of these, $C = 3\ kW/m^2$ en 20% mostly overestimates the distance, while $C = 5\ kW/m^2$ en 30% tends towards underestimating them. The parameters $C = 3\ kW/m^2$ and 30% or $C = 5\ kW/m^2$ and 20% give comparable results. Based on these results a choice was made for $A = 28150\ s \cdot \left(\frac{kW}{m^2}\right)^2$ (percentile value 20%), $B = 2$ and $C = 5\ kW/m^2$.

5.4 Sensitivity analysis of B

When B is lowered, the slope is more shallow. This would decrease the time to ignition for lower heat fluxes, while it increases them for higher heat fluxes. When fires with a low and a high heat flux are compared the distance to the reference dose would grow towards each other. When B is increased the opposite happens and the difference between a high and low heat flux fire would increase.

A sensitivity analysis was done to see if this effect occurs for the four incidents that were used. Table 4 and Table 5 show the distance to the reference dose for $B = 1.5$ and 2.5. $B = 1.5$ was chosen because this is what HSE uses.

Table 4 and Table 5 show a few things.

First is that $B = 1.5$ gives longer distances to the reference dose while $B = 2.5$ gives shorter distances. For $B = 1.5$ there are no cases where the distance to the reference dose is shorter than the lower estimate of the damage distance.

Using $B = 1.5$ or $B = 2.5$ would require other parameter sets. Because a comparison is made with the estimated damage distance of actual pipeline accidents, the distances to the reference dose remain more or less the same. Alternative parameter sets that can be use are, for example:

1. $B = 1.5, C = 5\ kW/m^2$, and 50%
2. $B = 1.5, C = 8\ kW/m^2$, and 10%
3. $B = 2.5, C = 5\ kW/m^2$, and 10%

These three alternatives are discussed in more detail in the appendix in Section 10.2. In short, the evaluation with the literature data of the first and third alternative is worse compared to the proposal. The second alternative results in distances with the largest deviation from the damage distance in the calibration.

Table 4 Distances (in meter) to the reference dose for different parameters for critical heat flux (C, kW/m^2) and percentile values, for B=1.5. For more details, see the caption of Table 3.

	San Bruno			**Sissonville**		
Damage distance (low)	150			130		
Damage distance (high)	180			165		
Distance to 10 kW/m2	321			292		
Distance HSE	211[c]			174[c]		
Distance DNV	184[c]			144[b]		
	C = 3	C = 5	C = 8	C = 3	C = 5	C = 8
10%	260[c]	242[c]	225[c]	232[c]	212[c]	193[c]
20%	225[c]	215[c]	208[c]	202[c]	186[c]	175[c]
30%	213[c]	204[c]	196[c]	192[c]	176[c]	164[b]
40%	204[c]	195[c]	189[c]	185[c]	169[c]	158[b]
50%	195[c]	189[c]	183[c]	177[c]	164[b]	152[b]

	Ludwigshafen			**Danville**		
Damage distance (low)	60			160		
Damage distance (high)	75			200		
Distance to 10 kW/m2	170			419		
Distance HSE	63[b]			184[b]		
Distance DNV	46[a]			134[a]		
	C = 3	C = 5	C = 8	C = 3	C = 5	C = 8
10%	146[c]	117[c]	86[c]	326[c]	277[c]	225[c]
20%	128[c]	104[c]	80[c]	271[c]	233[c]	198[b]
30%	120[c]	99[c]	75[b]	251[c]	217[c]	181[b]
40%	115[c]	94[c]	72[b]	236[c]	203[c]	172[b]
50%	108[c]	90[c]	69[b]	220[c]	193[b]	163[b]

[a] Shorter than the lower estimate of the damage distance
[b] Between the lower and higher estimate of the damage distance
[c] Longer than the higher estimate of the damage distance

Table 5 Distances (in meter) to the reference dose for different parameters for critical heat flux (C, kW/m^2) and percentile values, for B=2.5. For more details, see the caption of Table 3.

	San Bruno			**Sissonville**		
Damage distance (low)	150			130		
Damage distance (high)	180			165		
Distance to 10 kW/m2	321			292		
Distance HSE	211[c]			174[c]		
Distance DNV	184[c]			144[b]		
	C = 3	C = 5	C = 8	C = 3	C = 5	C = 8
10%	214[c]	212[c]	209[c]	183[c]	177[c]	172[c]
20%	201[c]	198[c]	197[c]	170[c]	163[b]	159[b]
30%	193[c]	192[c]	188[c]	162[b]	157[b]	150[b]
40%	185[c]	183[c]	181[c]	154[b]	149[b]	143[b]
50%	177[b]	175[b]	172[b]	147[b]	141[b]	135[b]

	Ludwigshafen			**Danville**		
Damage distance (low)	60			160		
Damage distance (high)	75			200		
Distance to 10 kW/m2	170			419		
Distance HSE	63[b]			184[b]		
Distance DNV	46[a]			134[a]		
	C = 3	C = 5	C = 8	C = 3	C = 5	C = 8
10%	96[c]	84[c]	69[b]	219[c]	202[c]	184[b]
20%	86[c]	75[b]	62[b]	195[b]	178[b]	163[b]
30%	80[c]	70[b]	57[a]	180[b]	168[b]	149[a]
40%	73[b]	64[b]	53[a]	165[b]	153[a]	138[a]
50%	67[b]	58[a]	47[a]	151[a]	139[a]	125[a]

[a] Shorter than the lower estimate of the damage distance
[b] Between the lower and higher estimate of the damage distance
[c] Longer than the higher estimate of the damage distance

5.5 Change of the distance to the reference dose in time

When using a dose relationship the distance to the reference dose will stay the same or increase in time. QRAs in the Netherlands are limited to scenarios with a maximum duration of 1800 seconds. A question is if the distance to the reference dose is still increasing after 1800 seconds. Figure 14 shows how the distance to the reference dose changes in time, as calculated using the results of Safeti-NL. On the x-axis is the distance to the fire, on the y-axis the time. For Danville it shows that after 1 minute materials will start to ignite at about 125 meter, after 200 seconds at about 170 meter. After 1000 seconds the distance to the reference dose has reached its maximum.

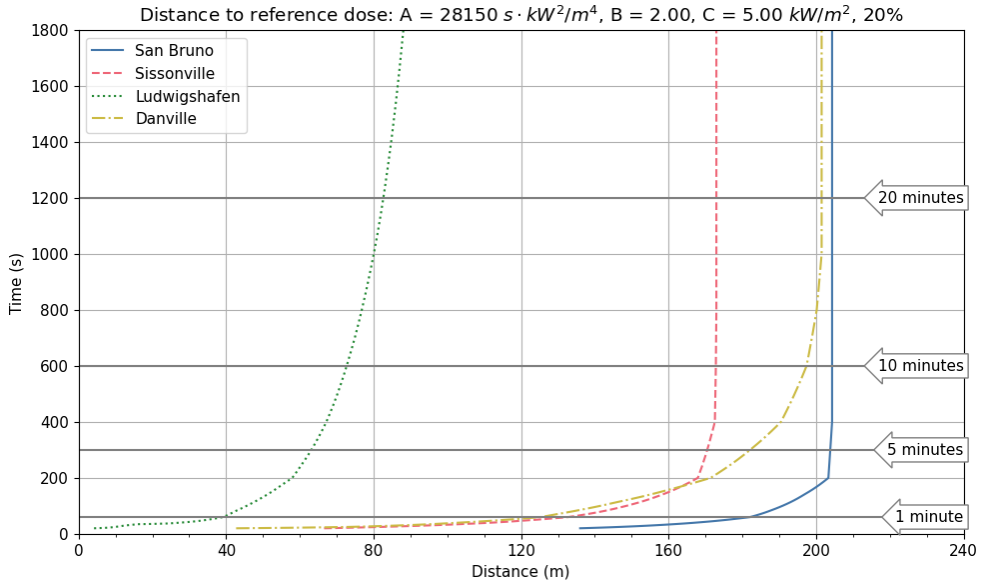

Figure 14 The distance to the reference dose in time for the four fires studied.

The figure shows two differences between the three fires in the US (San Bruno, Sissonville, and Danville) and the fire in Ludwigshafen. First, the distance to the reference dose is much larger for the American fires compared to the fire in Ludwigshafen. Second, the three fires in the US reached their maximum distance to the reference dose within 1000 seconds, while the distance to the reference dose continues to increase in Ludwigshafen. The difference is caused by the intensity of the fire and how it progressed in time.

Table 6 shows the time to ignition for the proposed dose relationship. The dose is reached much faster for high heat fluxes. Under 5 kW/m^2 the dose does not grow. For San Bruno, from the quick increase of the distance where the dose is reached, we can deduce the fire was very intense in the beginning.[11] After about five minutes the heat flux at ~200 meter had reduced to below 5 kW/m^2, meaning the distance did not grow further.

In Ludwigshafen the fire was not as intense as the fire in San Bruno. The distance to the reference dose grows much more slowly. Contrary to the fire in San Bruno, the intensity remained relatively high, meaning the distance continued to grow.

[11] This is slightly simplified because the height of the flame is also an important factor.

Table 6 Time to ignition for the dose relationship with A = 25150 s·(kW/m²)², B = 2 and C = 5 kW/m².

kW/m²	Time to ignition
6	7h 49m
8	52m
9	29m
10	19m
11	13m
13	7m 20s
15	4m 42s
20	2m 5s
30	45s
40	31s
50	14s

5.6 Discussion and conclusion

In this chapter the parameters A (reference dose), B (factor), and C (critical heat flux) of the dose relationship (Equation 3-1) were derived. As factor B was best defined it was derived first. Dose relationships for a range of values for C and A (using the percentage of data points below the curve) were compared to the literature data discussed in the previous chapter and model calculations of actual accidents of pipeline ruptures. $A = 28150\ s \cdot (kW/m^2)^2$ (percentile value 20%), $B = 2$ and $C = 5\ kW/m^2$ gives the best conservative description of the damage observed in the four studied incidents.

All parameters are dependent on the literature data available. Additional data will result in different parameters. More experimental data below 10 kW/m² would make a better estimate of the critical heat flux possible. More experimental data may also change factor B. More information about the damage from the pipeline fires would result in a more accurate estimate of the damage distance, although this was solved by using a minimum and maximum estimate. However, by using two complementary types of information, both experimental results and accident case studies, the reliability of the results is increased.

Table 3, Table 4, and Table 5 show the sensitivity of the calculation to the parameters. Different values for B, C, and the percentile result in different distances. The differences were however not large enough to consider adding additional in-between values for B and C.

In this literature study a conservative choice was made to only use piloted ignition data. The calibration with actual accidents makes the end result a realistic worst-case approximation instead of being overly conservative.

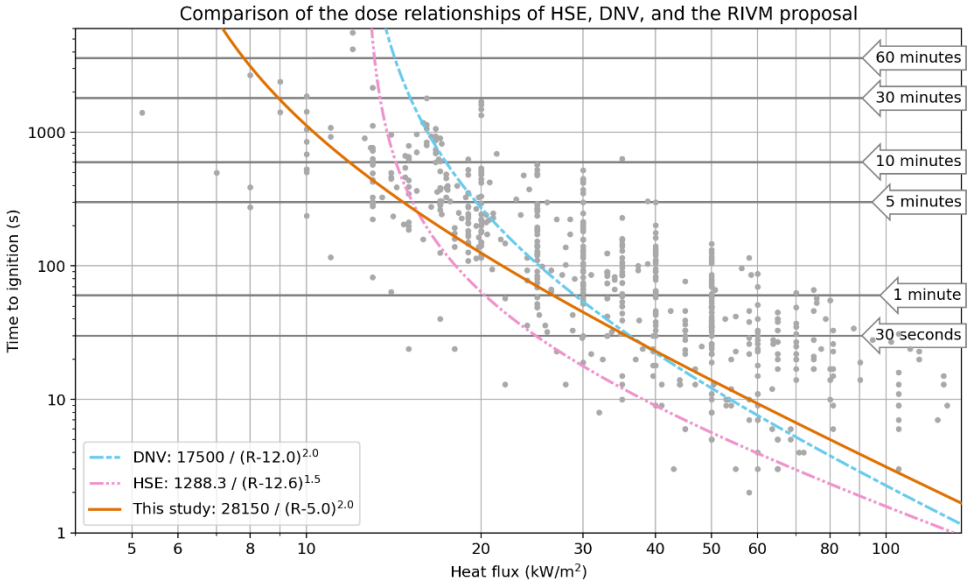

Figure 15 Comparison of the dose relationships by DNV, HSE, and this study.

Figure 15 and Table 7 show a comparison of our dose relationship and those of DNV and HSE. Above 30 kW/m^2 our result is more or less comparable to that of DNV. The calculations of the dose for the accidents shows that DNV significantly underestimates the distance to the damage distance. This shows how important the contribution of the lower heat fluxes to the dose is.

Table 7 Time to ignition for the dose relationships in this study, DNV, and HSE, in seconds.

kW/m²	**This study**	**DNV**	**HSE**
6	28200		
8	3130		
9	1760		
10	1130		
11	782		
13	440	17500	5090
15	282	1940	346
20	125	273	64
30	45	54	18
40	23	22	9
50	14	12	6
60	9	8	4

6 Comparison of the current and proposed method to calculate the fire focus area

The fire focus areas are currently bound by the distance where the heat flux is equal to 10 kW/m^2, irrespective of the time duration. In paragraph 5.6 a dose relationship is proposed, where the fire focus area is bound by the distance where:

$$\int (R - C)^B dt = A$$

with A = 28150 s·(kW/m^2)^2, B = 2 and C = 5 kW/m^2. In this chapter the fire focus areas are calculated using Safeti-NL for various example scenarios, using both the current and proposed method. The scenarios include cases where the heat flux is considered constant (pool fire and jet fire), a dynamic case (high pressure natural gas pipeline rupture), and a short-duration fire (fireball). The comparison of the two methods is to illustrate the effect on the distance to the boundary of the focus area. Different parameters will lead to different results.

6.1 A constant heat flux

Table 8 shows different combinations of heat flux and fire durations at which the reference dose is reached. For example, at a constant heat flux of 10 kW/m^2 the reference dose will be reached after 1130 seconds. Compared to the current method, this means that for fires longer than 1130 seconds the fire focus area will increase, while for fires shorter than 1130 seconds it will decrease.

Table 8 The heat flux corresponding to the reference dose A for fire durations

Fire duration	Heat flux
20 s	43 kW/m^2
60 s	27 kW/m^2
600 s	11.8 kW/m^2
1130 s	10.0 kW/m^2
1800 s	9.0 kW/m^2
3600 s	7.8 kW/m^2

6.1.1 Pool fire

The maximum duration of a pool fire in Safeti-NL 8.8 is 1800 s. Table 8 shows that for an exposure time of 1800 s, a heat flux of 9.0 kW/m^2 is needed to reach the reference dose.

The distance to 10 kW/m^2 and the reference dose A is for pool fires shown in Table 9.

Table 9 Distances to heat flux 10 kW/m² and the reference dose A for some example pool fires (pool fire diameter 50 m, duration 1800 s, weather class D9).

Material	Heat radiation 10 kW/m²	Reference dose A	Difference
hexane	41 m	47 m	15%
propane	149 m	155 m	4%
methane	176 m	183 m	4%

The proposed method results in a 4 – 15% increase in the distance to the boundary of the fire focus area.

6.1.2 *Horizontal jet fire*

To illustrate the consequences for a jet fire, the heat radiation of a horizontal jet fire is calculated for a release of a 50 tonnes tank wagon filled with propane through a hole of 75 mm. The flow rate is equal to 64 kg/s, the duration of the outflow is equal to 780 s. With an exposure time of 780 s a constant heat flux of 11.0 kW/m² is needed to reach the reference dose.

The distance to 10 kW/m² and the reference dose A are shown in Table 10.

Table 10 Distances to heat flux level 10 kW/m² and the reference dose A for an example jet fire of propane (duration 780 s, weather class D9).

Material	Heat radiation 10 kW/m²	Reference dose A	Difference
propane	117 m	115 m	-2%

With the proposed method there is a 2% decrease in the distance to the boundary of the fire focus area.

6.2 Dynamic heat flux: high pressure natural gas pipeline

The fire focus area for a high pressure natural gas pipeline with a 42 inch diameter and 66.2 bar was calculated using Safeti-NL 8.8. The results are shown in Table 11.

Table 11 Distances to 10 kW/m² calculated with Safeti-NL and the reference dose A for an example high pressure natural gas pipeline (H-gas[12], weather class D9).

Pipeline	Heat radiation 10 kW/m²	Reference dose A	Difference
42”, 66 bar	679 m	456 m	-33%

Using the reference dose A instead of the heat radiation 10 kW/m², there is a 33% decrease in the distance to the boundary of the fire focus area.

The calculation of the reference dose is done for a time period of 1800 s. The distance to the reference dose will only grow when the heat flux is above 5 kW/m² (the critical heat flux C). After 1800 seconds the heat

[12] The tabulated distance to 10 kW/m² is calculated with H-gas, and therefore the Safeti-NL calculation is also done for H-gas. H-gas is high-calorific natural gas that contains relatively large proportions of higher hydrocarbons and consequently has more energy than low-calorific gas. H-gas › Gasunie

flux at 456 meter is below 5 kW/m^2. This means that the distance to the reference dose will not grow anymore after 1800 s.

6.2.1 *Comparison between Safeti-NL and Carola*

Currently the fire focus area for high pressure natural gas pipelines is given in tabular form[13]. These values are the distance to 10 kW/m^2 as calculated with the software package CAROLA [35] and based on the model PIPESAFE. For a pipeline with diameter 42 inch and pressure 66.2 bar, the distance to the boundary of the fire focus area is 485 m. This tabulated distance is now used as the focus area.

The distance to the heat radiation of 10 kW/m^2 as calculated with Safeti-NL, 679 m, is 40% larger than the distance calculated with CAROLA, 485 m. This is caused by differences in the jet fire modelling between Safeti-NL and PIPESAFE[14]. CAROLA can not be used to calculate the focus area with the proposed method.

6.3 Short-duration fire: fireball

A fireball is a short duration event, typically 10 – 20 s. For such a short duration event, the focus area[15] is currently bounded by the distance to a heat radiation of 35 kW/m^2. To illustrate the consequences of the dose approach, the heat radiation of a fireball is calculated for a 50 tonnes tank wagon filled with propane using Safeti-NL.

The duration of the fireball is 13.5 s, the radius is 107 m and the distance to 35 kW/m^2 is equal to 272 m.

The heat radiation of a fireball varies in time as the fireball grows and lifts off. Safeti-NL 8.8 does give distance versus the maximum heat flux, but not the time varying heat flux needed for the dose calculation. Using the dose relationship, the reference dose is reached after the duration of the fireball, 13.5 s, for a continuous heat flux of 50 kW/m^2. A maximum heat flux of 50 kW/m^2 corresponds to a distance of 224 meter. Because the maximum heat flux was used, this is an overestimation of the dose at 224 m and the actual fire focus area will be smaller.

The results are summarized Table 12.

Table 12 Distances to heat flux 35 kW/m^2 and the reference dose A for a fireball of 50 tonnes propane (fireball duration 13.5 s).

Material	Heat radiation 35 kW/m^2	Reference dose A
propane	272 m	≤ 224 m

Using the reference dose A instead of the heat radiation for short duration events, 35 kW/m^2, there is a 18% or more decrease in the distance to the boundary of the fire focus area.

[13] https://www.rivm.nl/omgevingsveiligheid/handboek/stappenplannen/bepalen-afstanden-en-gebieden/brandaandachtsgebied
[14] An analysis of the differences in jet fire modelling between Safeti-NL and PIPESAFE is not part of this project.
[15] For fireballs, the focus area is called an explosion focus area to emphasize the character of the phenomenon

6.4 Conclusions

Using the reference dose A as the boundary of the fire focus area instead of the 10 kW/m^2 boundary will increase the focus area for fires with constant intensity lasting more than 1130 seconds. In the examples this is illustrated by three pool fires where the focus area increases slightly. On the other hand, the example with the 780 second jet fire illustrates that for shorter duration fires the focus area will decrease.

The dose relationship can be used to calculate the focus area of fireballs, but at this moment the result had to be approximated because Safeti-NL does not report the heat flux variation over time. In the example the focus area decreases significantly.

In line with the results of the accidents described in Section 5.3 the example with the high pressure natural gas pipeline shows a significantly shorter distance to the boundary of the fire focus area when using the dose relationship, compared to the Safeti-NL calculation for the 10 kW/m^2 boundary.

7 Conclusions

The goal of this study was to develop a new method to calculate the fire focus area. After studying various threats of fire, the initiation of secondary fires due to radiation was considered to be the most relevant.

A dose relationship was derived based on literature data and calibrated using four pipeline accidents. Compared to dose relationships used by HSE and DNV the dose relationship proposed in this report results in damage distances that are larger, but match the damage seen in pipeline accidents better. A major difference is a much lower critical heat flux C of 5 kW/m^2 instead of 12.6 kW/m^2 and 12.0 kW/m^2, for HSE and DNV respectively. Both HSE and DNV based their critical heat flux (mostly) on wood, while this report also considers plastics and other materials.

Using the dose relationship derived in this report gives a better approximation of the effect zone where an incident can have life-threatening consequences for people inside buildings compared to the calculations based on heat flux.
The calculated area is more realistic for short fires and fires where the intensity varies in time, and is approximately the same for pool and jet fires with typical durations in the order of 600 - 1800 s.

8 Appendix: literature study

8.1 Literature search

Two literature searches have been done, once at the end of 2021 and once during the summer of 2023.

8.1.1 Search 2021

A search was done on Scopus, using:

- (Set 1 OR set 2 OR set 3 OR set 4 OR set 5)
- (Set 1 OR set 2 OR set 3 OR set 4 OR set 5) AND set 6

485 articles were found, 348 of them published after 2000. Only the articles after 2000 were considered.

Table 13 An overview of the search terms used to search Scopus during the 2021 literature search.

Set	Search terms
1	TITLE("piloted ignition")
2	TITLE(("combustibil*") AND ("hous*" OR "material*" OR "building*" OR "wood*"))
3	TITLE-ABS-KEY-AUTH(("piloted ignition") AND ("hous*" OR "material*" OR "building*" or "wood*"))
4	TITLE(("ignit*") AND ("hous*" OR "material*" OR "building*" or "wood*"))
5	TITLE(("radiat*" OR "convect*" OR "conduct*") AND ("ignit*") AND ("hous*" OR "material*" OR "building*" or "wood*"))
6	PUBYEAR > 2000

8.1.2 Literature search 2023

In 2023 a second literature search was done. This search focussed more on piloted ignition than specific materials.

A search was done on Scopus, using search terms:

- (Set 1 OR set 2 OR set 3 OR set 4 OR set 5) AND set 6

This resulted in 54 articles.

Table 14 An overview of the search terms used to search Scopus during the 2023 literature search.

Set	**Search terms**
1	TITLE-ABS-KEY-AUTH ("piloted ignit*") AND TITLE-ABS-KEY-AUTH ("transient radiat*" OR "transient irradiat*" OR "transient heat*")
2	TITLE-ABS-KEY-AUTH ("piloted ignit*") AND TITLE-ABS-KEY-AUTH ("transient*")
3	TITLE-ABS-KEY-AUTH ("piloted ignit*") AND TITLE ("ignition model*" OR "ignition time*")
4	TITLE-ABS-KEY-AUTH ("piloted ignit*") AND TITLE ("heat flux*" OR "heat transfer*")
5	TITLE-ABS-KEY-AUTH ("transient radiat*" OR "transient irradiat*" OR "transient heat*") AND TITLE-ABS-KEY-AUTH ("combustib*")
6	PUBYEAR > 1999 AND PUBYEAR < 2024

An additional search was done on Embase.com using the search term:

- 'piloted ignit*':ti,ab AND [2000-2023]/py

This yielded 14 articles.

A detailed list of data sources and all data points can be found in the appendix in Chapter 11.

8.2 Dose relationships by DNV and HSE

Both DNV and HSE use slightly different versions of the dose relation in Equation 3-1.

DNV used

$$t_{ig} = A(R - C)^{B'} \qquad 8\text{-}1$$

which is equivalent to Equation 3-1, where $B' = -B$.[5]

Bilo et al and HSE use

$$t_{ig} = \left(\frac{A'}{R - C}\right)^{B} \qquad 8\text{-}2$$

With $A = (A')^B$ this is equivalent to Equation 3-1. Bilo et al find $A' = 118.4\ s \cdot kW/m^2$ or $A = 1288\ s \cdot (kW/m^2)^{1.5}$, $B = 1.5$ and $C = 14.7\ kW/m^2$.[6]

In their 2006 review of ignition criteria HSE however uses a different critical heat flux of 12.6 kW/m^2, while leaving the other parameters equal.[8] In this report the dose relationship with $A = 1288\ s \cdot (kW/m^2)^{1.5}$, $B = 1.5$ and $C = 12.6\ kW/m^2$ is referred to as "HSE".

8.3 Data sets

Section 3.3.1 shows data sets for pine and PMMA. A data set is a collection of measurements where all parameters stay the same, except for the heat flux. This section contains additional plots for more materials. In some cases a few materials have been grouped. In these plots the proposed dose relationship is included, which is why figures for pine and PMMA are included again.
In some cases a single heat flux was measured more than once. In these cases these data points were averaged. This is indicated by an asterisk in the legend entry.

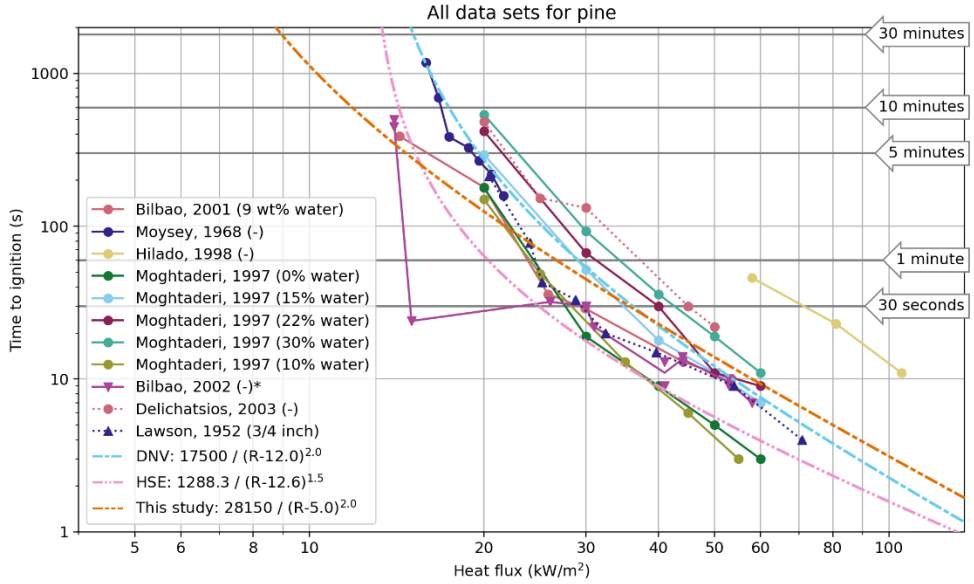

Figure 16 Data sets for pine. The asterisk in the legend means several data points with the same heat flux were averaged.

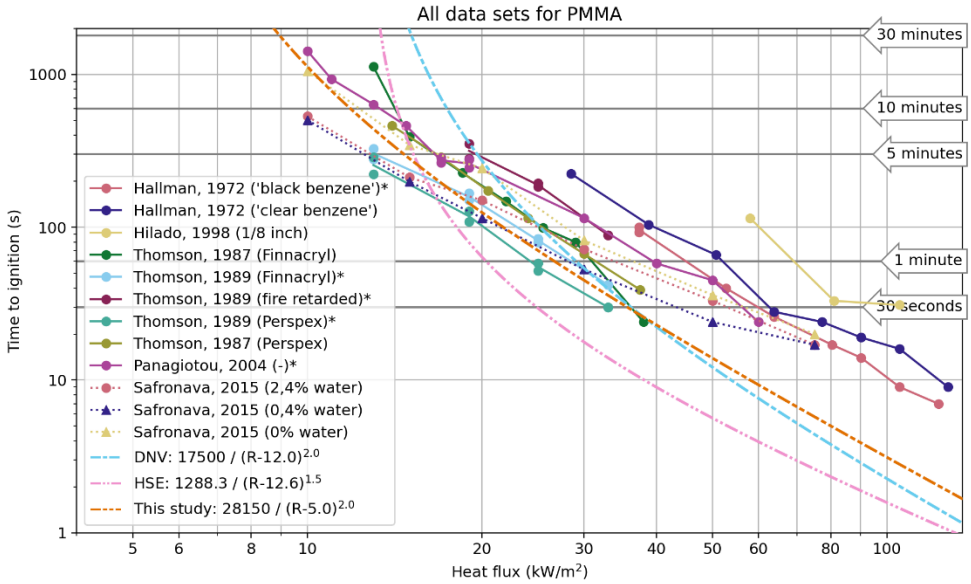

Figure 17 Data sets for PMMA. The asterisk in the legend means several data points with the same heat flux were averaged.

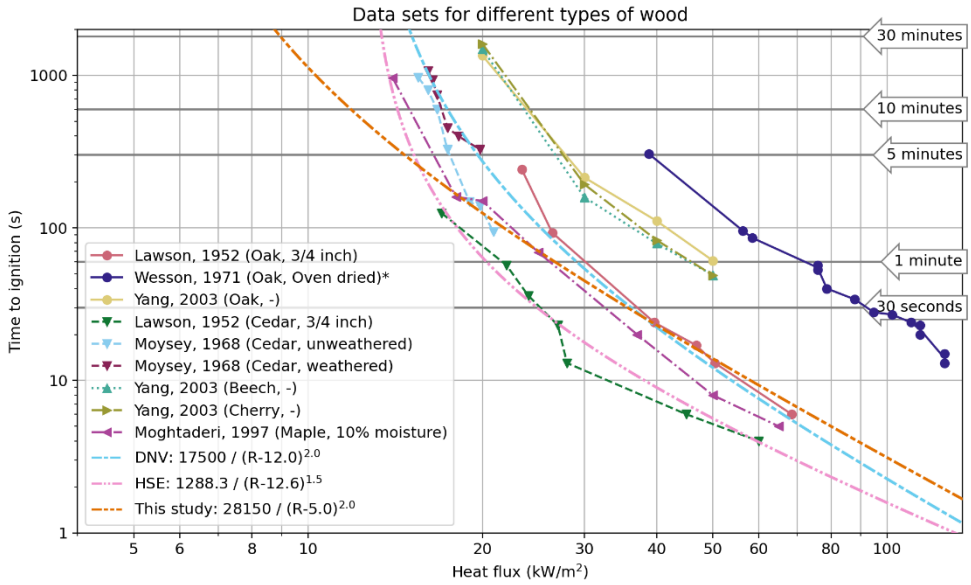

Figure 18 Data sets of different types of wood. The asterisk in the legend means several data points with the same heat flux were averaged.

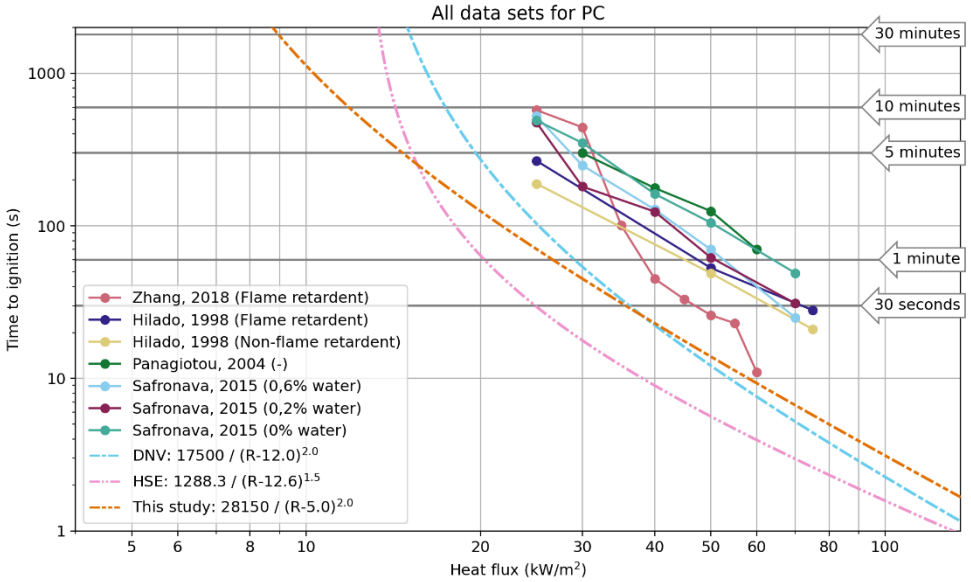

Figure 19 Data sets of polycarbonate (PC)

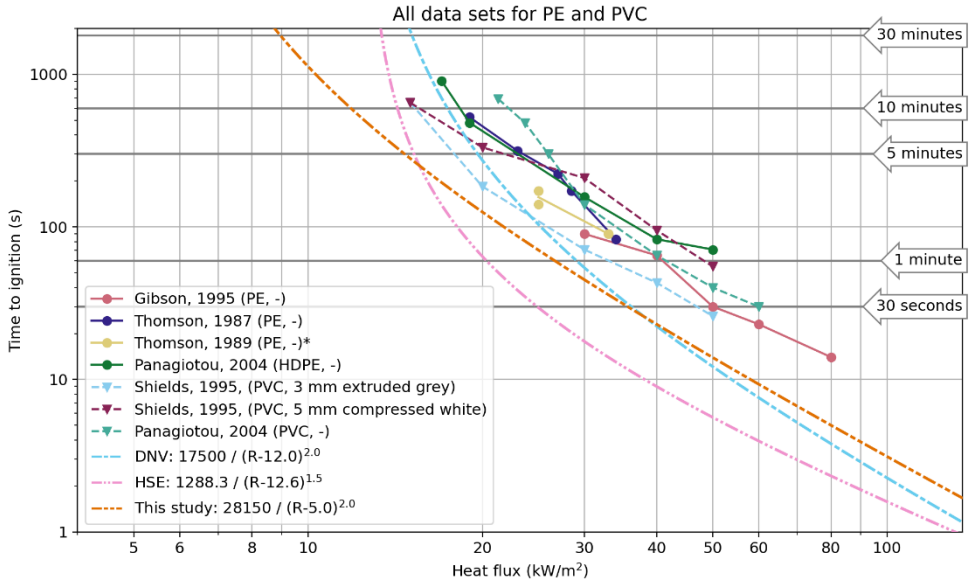

Figure 20 Data sets of polyethylene (PE) and PVC. The asterisk in the legend means several data points with the same heat flux were averaged.

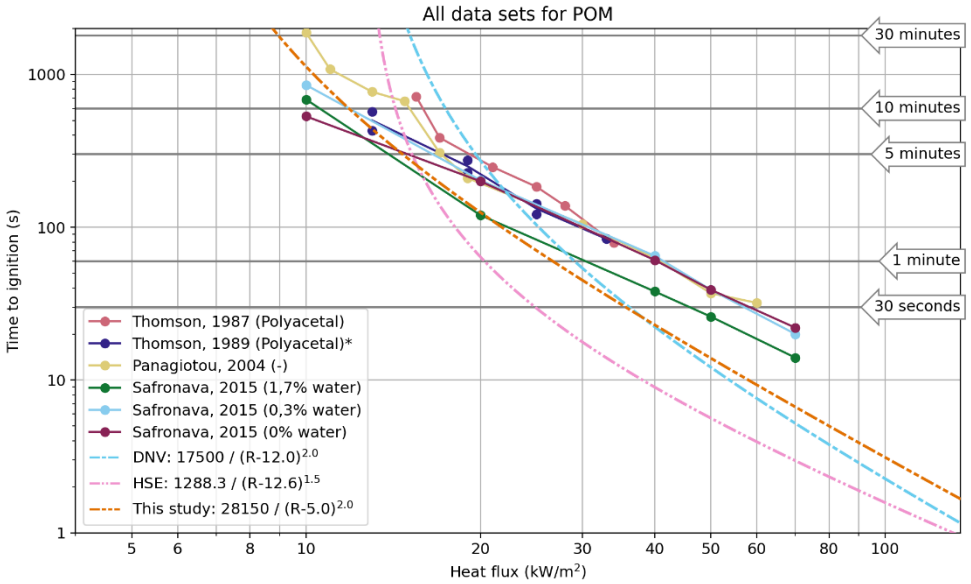

Figure 21 Data sets of POM. The asterisk in the legend means several data points with the same heat flux were averaged.

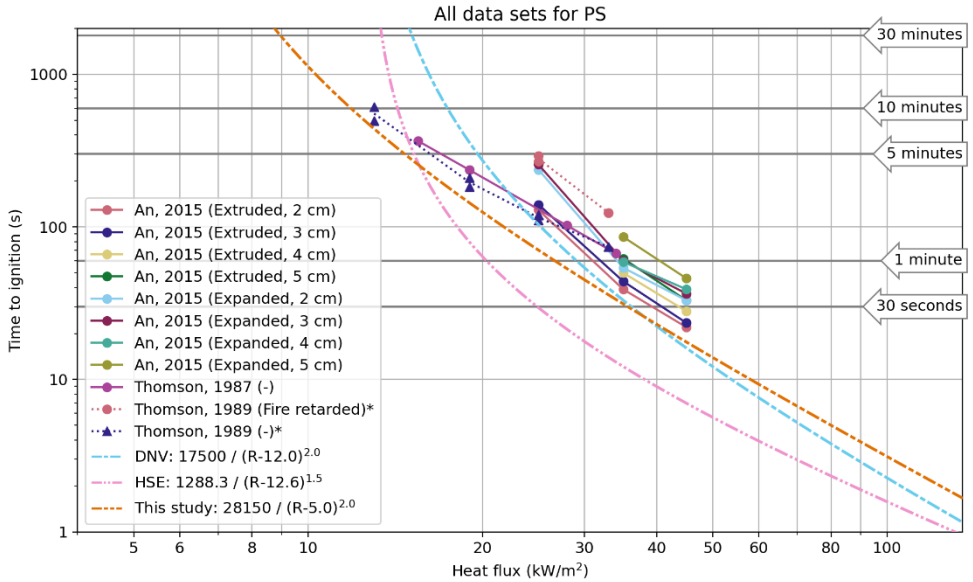

Figure 22 Data sets of polystyrene (PS). The asterisk in the legend means several data points with the same heat flux were averaged.

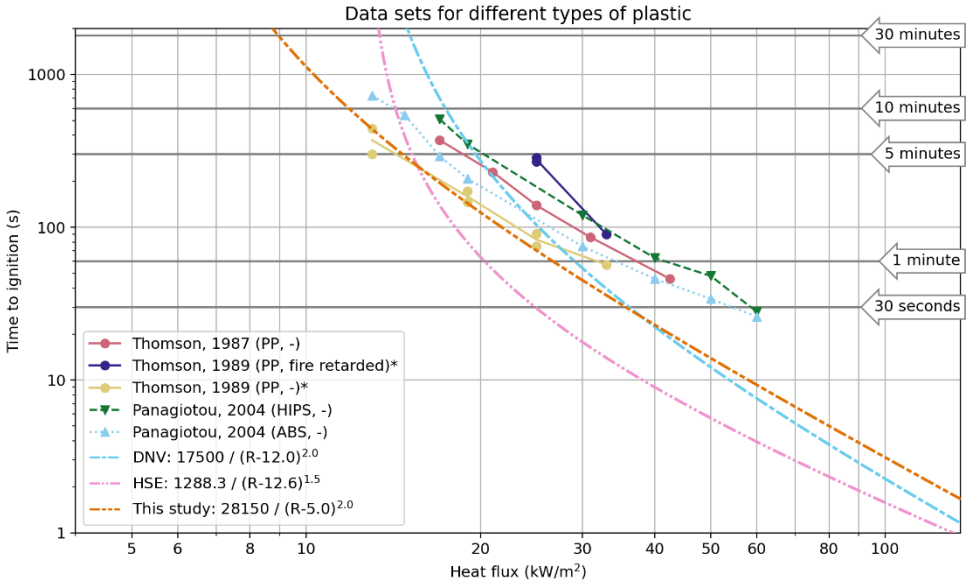

Figure 23 Data sets of different types of plastic. The asterisk in the legend means several data points with the same heat flux were averaged.

9 Appendix: derivation of the dose relationship

In Section 4.2 the general method of the derivation of the dose relationship was explained. In Section 4.3 the results were summarized. In this appendix the derivation of the dose relationship and the evaluation of the results are described in more detail.

In short, factor B was determined by fitting all data to the dose relationship with $C = 0\ kW/m^2$. Then a range of values for the critical heat flux C was chosen (3, 5 and 8 kW/m^2). For a large number of values for A the percentage of datapoints below the dose relationship (i.e. igniting before the dose relationship predicts) was determined. The values for A closest to few chosen percentile values (10, 20, 30, 40, and 50 percent) were used as the reference dose.

The results were then evaluated against the literature data. The criteria are explained in Section 9.1, the results are shown in Section 9.2.

9.1 Criteria to evaluate the dose relationship using literature data

For each combination of percentile value (A) and C the result was evaluated using the literature data in two ways, the number of data points below the curve, and the root mean square difference between the data points and the curve. The evaluation was done for all data points together, but also for low and high heat fluxes separately. As discussed in Section 3.3.1, below 20 kW/m^2 plastics ignites earlier than wood, while above 20 kW/m^2 it is the other way around. This seemed like a natural point to divide low and high heat flux. At or above 20 kW/m^2 is considered high heat flux[16], below 20 kW/m^2 is considered low heat flux.

9.1.1 Number of data points below the curve

When a data point is below the curve it means it will ignite earlier than calculated by the dose relationship. The percentile value determines the total number of points below the curve.

When $R \leq C$ (i.e. the heat flux R is at or below the critical heat flux C) that data point is also considered to be "below the curve". The lowest heat flux in the data set was 5.2 kW/m^2.

9.1.2 Root mean square difference

The root mean square (RMS) of the difference between the curve and the datapoints below the curve was calculated using the following equation:

$$RMS = \sqrt{\frac{1}{n}\sum_i^n \left[\log_{10}\left(t_{ig}(data)\right) - \log_{10}\left(t_{ig}(curve)\right)\right]^2} \qquad 9\text{-}1$$

[16] For brevity "at or above" is called "above"

Like in Figure 2 a logarithmic scale is used. In this case data points $R \leq C$ are *not* included in the result.

Although data at or below the critical heat flux is not included in the calculation, a value just above the critical heat flux may distort the result. At this point the calculated time to ignition will still be very high. This should be considered when comparing the RMS.

9.2 Results of determining reference dose A

This section shows the results of the calculation of the reference dose. The calculations were done for C = 3, 5, and 8 kW/m^2, with percentile values between 10-50%. The results are presented in figures and tables showing the results of the evaluation criteria described in Section 9.1. The evaluation was meant to quantify the differences between the different dose relationships, but they should be interpreted in conjunction with the figures.

N<20 and ***N≥20*** show the number of points below the curve for the low and high heat flux regions. Because the reference dose A was increased in steps, the sum of *N<20* and *N≥20* is not always the same at the different percentile values. The actual percentage varies by +/- 0.2%, except for C = 5 kW/m^2 at 10%, where it actually is 10.4%. These differences were not considered significant.

N ratio is the ratio of *N≥20* divided by *N<20.* There is not an ideal ratio. Of the 605 datapoints 142 are <20 kW/m^2, while 463 are ≥20 kW/m^2, 3.3 times more.[17] On the other hand, most of the data for processed wood and the outlier is in the low heat flux area. Since these points are always below the curve, the ratio is generally below 3.3.

RMS<20 and ***RMS≥20*** show the root means square difference for the low and high flux regions. ***RMS ratio*** is the larger of the two divided by the smaller one. The value is thus always 1 or above. ***RMS all*** shows the RMS for all data.

9.2.1 Results for C = 3 kW/m^2

Table 15 Results of the evaluation for C = 3 kW/m^2

C = 3 kW/m2	10%	20%	30%	40%	50%
A	21900	35800	50700	60400	75200
N <20.0	11	31	52	72	92
N >=20.0	49	91	129	170	211
N ratio	4.5	2.9	2.5	2.4	2.3
RMS <20.0	0.497	0.430	0.428	0.413	0.429
RMS >=20.0	0.262	0.340	0.398	0.403	0.432
RMS ratio	1.9	1.3	1.1	1.0	1.0
RMS all	0.318	0.365	0.407	0.406	0.431

[17] 16 datapoints are <10 kW/m^2

Table 15 and Figure 24 show the results for C = 3 kW/m^2. Of note is that for 10% the ratios for both N and RMS are significantly higher than for the other percentile values.

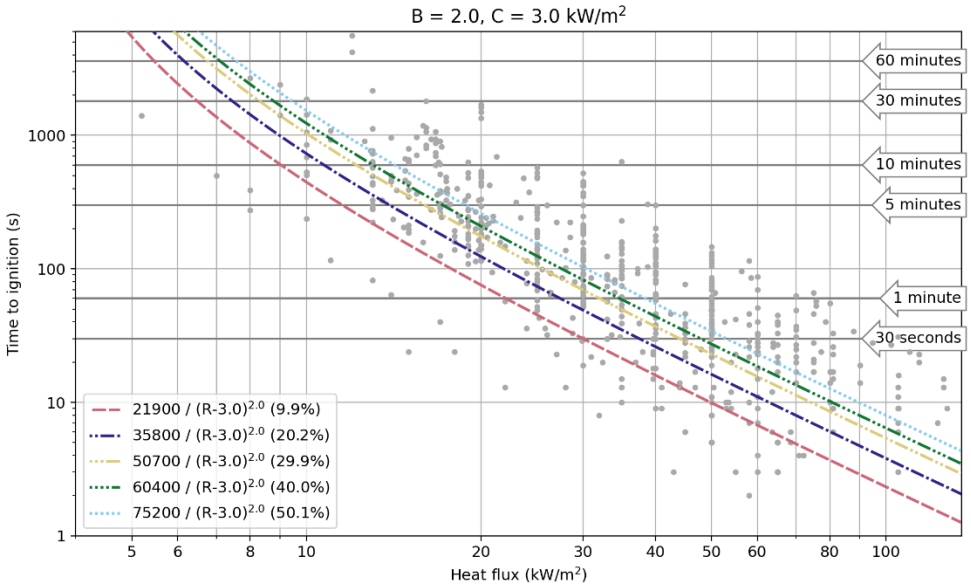

Figure 24 Results for B = 2 and C = 3 kW/m^2, for different percentile values.

9.2.2 *Results for C = 5 kW/m^2*

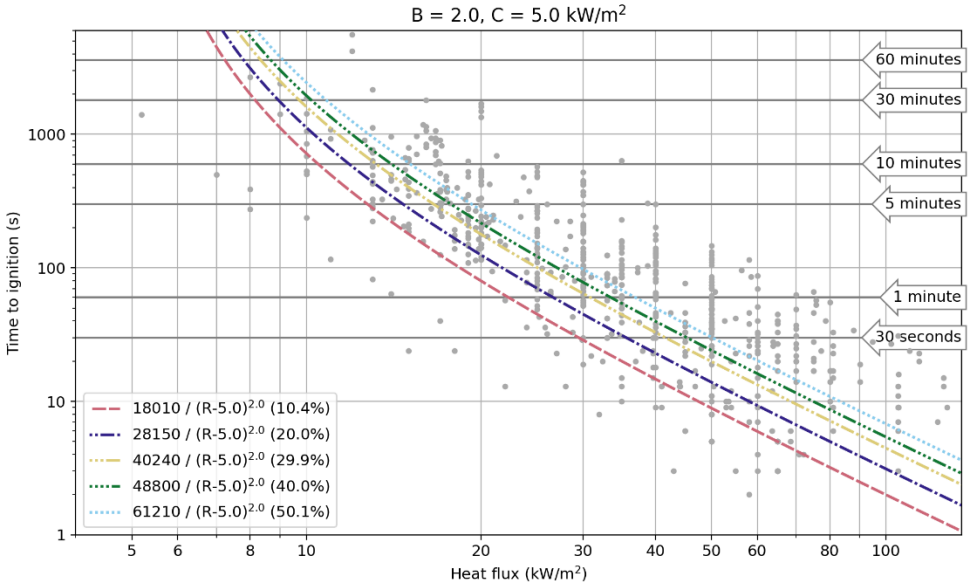

Figure 25 Results for B = 2 and C = 5 kW/m^2, for different percentile values.

Table 16 and Figure 25 show the results for C = 5 kW/m^2. The RMS values below 20 kW/m^2 are very high. This is caused by a single data point at 5.2 kW/m^2 because the curve is going to infinite at 5 kW/m^2. Removing this data point (or other data points) does not influence the results for C=3 and 8 kW/m^2 as much.

Table 16 Results of the evaluation for C = 5 kW/m²

C = 5 kW/m2	10%	20%	30%	40%	50%
A	18010	28150	40240	48800	61210
N <20.0	18	38	65	87	101
N >=20.0	45	83	116	155	202
N ratio	2.5	2.2	1.8	1.8	2.0
RMS <20.0	0.787	0.647	0.579	0.549	0.572
RMS >=20.0	0.246	0.310	0.378	0.389	0.413
RMS ratio	3.2	2.1	1.5	1.4	1.4
RMS all	0.469	0.445	0.461	0.453	0.472

Table 17 Statistics for $C = 5\ kW/m^2$, where the datapoint at $R = 5.2\ kW/m^2$ has been removed.

C = 5 kW/m2	10%	20%	30%	40%	50%
A	*18010*	*28160*	*40270*	*48810*	*61790*
N <20.0	*17*	*37*	*65*	*86*	*100*
N >=20.0	*45*	*84*	*116*	*156*	*202*
N ratio	*2.6*	*2.3*	*1.8*	*1.8*	*2.0*
RMS <20.0	*0.536*	*0.483*	*0.459*	*0.453*	*0.491*
RMS >=20.0	*0.246*	*0.309*	*0.378*	*0.388*	*0.416*
RMS ratio	*2.2*	*1.6*	*1.2*	*1.2*	*1.2*
RMS all	*0.350*	*0.371*	*0.409*	*0.412*	*0.442*

Table 17 shows the results with this single data point removed. The RMS all and RMS <20 kW/m² are significantly smaller. Note that the results in Table 17 are from a completely different calculation, where also new values for A have been determined. This also causes small differences in the value of RMS >20 kW/m².

9.2.3 *Results for C = 8 kW/m²*

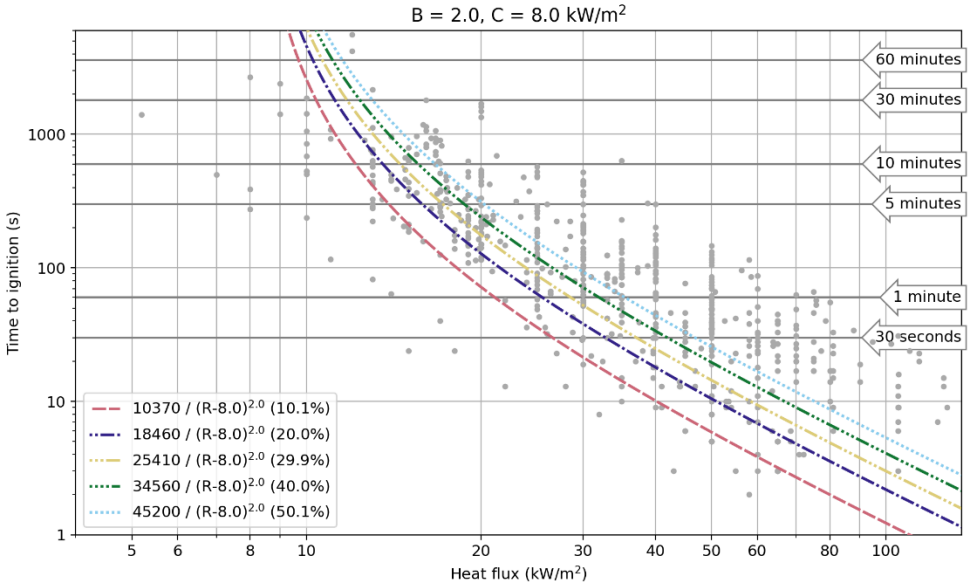

Figure 26 Results for B = 2 and C = 8 kW/m², for different percentile values.

Table 18 and Figure 26 show the results for C = 8 kW/m².

As explained above there are 3.3 times more data points in the high flux region. With an *N ratio* close to 1 – and for 10% actually 0.7 – this means relatively many data points in the low flux region are below the curve. This is also clear from the figure, where for example all data points at or below 10 kW/m² are below the curve. This is not the case for C = 3 and 5 kW/m².

Table 18 Results of the evaluation for C = 8 kW/m²

C = 8 kW/m2	10%	20%	30%	40%	50%
A	10370	18460	25410	34560	45200
N <20.0	36	58	84	105	117
N >=20.0	25	63	97	137	186
N ratio	0.7	1.1	1.2	1.3	1.6
RMS <20.0	0.512	0.557	0.548	0.579	0.633
RMS >=20.0	0.202	0.275	0.318	0.365	0.399
RMS ratio	2.5	2.0	1.7	1.6	1.6
RMS all	0.404	0.427	0.436	0.467	0.500

9.2.4 *Comparing the results for the three critical heat fluxes*

In the previous paragraphs the results for one C for different percentage values were presented. Figure 27 shows how the dose relationship changes for a fixed percentile value (20%) for the three critical heat fluxes. Although only this figure is shown, the discussion in this section is applicable to all percentile values.

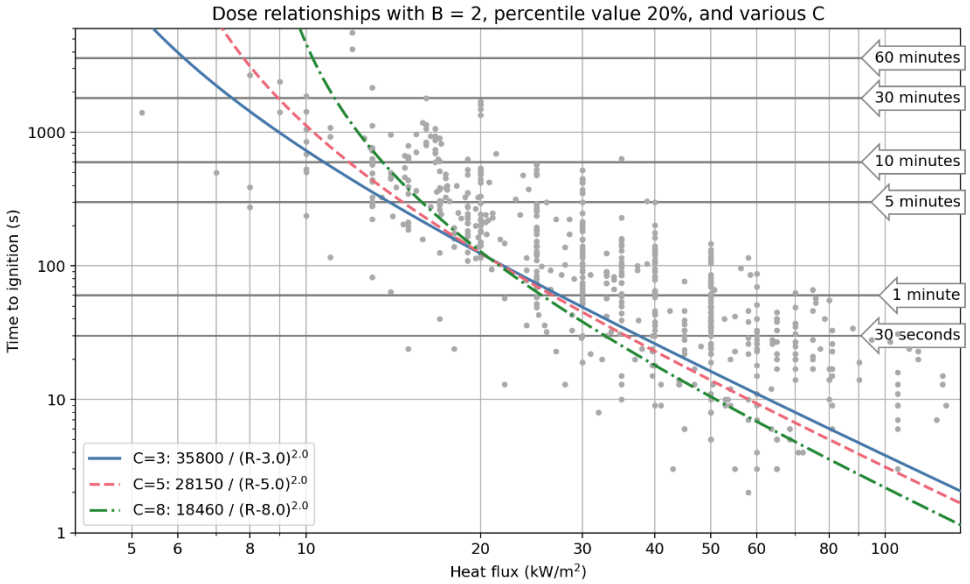

Figure 27 Results for B = 2 and a percentile value of 20%, for different critical heat fluxes.

In Figure 24 to Figure 26 it was clear that for a higher percentile value the dose would be higher and the time to ignition would increase. When the critical heat flux is varies, as in Figure 27, this is more complex. The reference dose can't be compared directly because the denominator is different.

It is noticeable that for higher critical heat fluxes the time to ignition is longer for low heat fluxes and shorter for high heat fluxes. The reason is that for higher critical heat fluxes there are more points below the curve at low heat fluxes and, to fulfil the requirement of the 20% percentile, fewer points can be below the curve at higher heat fluxes. This also result in a higher *RMS ratio* for C = 8 kW/m^2 than for C = 3 kW/m^2 and 5 kW/m^2 (Table 15 and Table 17).

Figure 27 makes clear how many data points at low heat fluxes are below the curve for C = 8 kW/m^2 compared to C = 3 kW/m^{2}and 5 kW/m^2.

In most cases the *N ratio* is around 2. This means relatively more data points in the low flux area are below the curve. For percentile value of 40% this means that 51 to 74% of the data points in the low flux region is below the curve. For the 50%-percentile this is 65 to 82%.

For C = 3 kW/m^2 and 5 kW/m^2 the 10%-percentile has a higher *N ratio* than the other percentiles.

9.2.5 *Discussion and conclusions*

This section presented the results of the calculation of reference dose A, and how the result was evaluated using two criteria. These evaluation criteria proved useful to quantitatively compare the results, but can not be used to select a particular dose relationship.

From the results in this chapter C = 3 and 5 kW/m^2 agree better with the literature data than C = 8 kW/m^2.

10 Appendix: calibration with pipeline accidents

10.1 Input parameters

Below are the input parameters used for the Safeti-NL calculations. Not all parameters were known. In these cases a value was assumed. If no weather information was available, the defaults used in the Netherlands were chosen (ground temperature 10 C, stability D, wind speed 5 m/s). Historical weather data is available, but this is usually for distant weather stations (Sissonville: 15 km) and large time spans (6 hours, or the daily average).

10.1.1 San Bruno

Parameter	Value	Unit	Source
Material	Methane		Report (natural gas)
Temperature	15.5	C	Report, section 1.5
Pressure	26.6	bar	Report, section 1.1.3
Diameter	743	mm	Report, section 1.8
Wind speed	9	m/s	Report, section 1.5
Weather type	D		Based on time of day and cloud cover (1/8 to 4/8)
Wind direction	WNW		Report, section 1.5
Pumped inflow	17.5	kg/s	Operations Factual Report Addendum-Redacted
Fracture length	8.53	m	Report, section 1.1
Relative size	1		
Depth	1.5	m	Report, figuur 16
Soil type	Clay		Safeti-NL default

10.1.2 Sissonville

Parameter	Value	Unit	Source
Material	Methane		Report (natural gas)
Temperature	10	C	Assumption
Pressure	64.05	bar	Report p20, 929 psig
Diameter	494	mm	
Wind speed	5	m/s	Assumption
Weather type	D		Assumption
Wind direction	Unknown		
Pumped inflow	20	kg/s	Assumption
Fracture length	6.1	m	Report p11, 20 feet
Relative size	1		
Depth	1.2	m	2 feet deep on one side, 6 feet on the other side. Average of 4 feet is used.
Soil type	Clay		Safeti-NL default

10.1.3 *Ludwigshafen*

Parameter	Value	Unit	Source
Material	Methane		Report (natural gas)
Temperature	10	C	Assumption. A nearby weather station report an air temperature of 11 C and a soil temperature at 100 cm depth: 16.0 C
Pressure	60	bar	Assumption, max pressure is 67 bar (Marc Dröge, Gasunie)
Diameter	400	mm	Gasunie
Wind speed	1.5	m/s	Weather station 1.3 m/s
Weather type	D		Cloud coverage 8/8
Wind direction	220	degrees	Weather station
Pumped inflow	100	kg/s	Assumption
Fracture length	12	m	Default
Relative size	1		
Depth	2	m	Photographs
Soil type	Clay		Default

10.1.4 *Danville*

Parameter	Value	Unit	Source
Material	Methane		Report (natural gas)
Temperature	10	C	Assumption
Pressure	63.8	bar	Report, Section 1.4.1
Diameter	743	mm	Report, Section 1.4.1
Wind speed	1.5	m/s	Meteo appendix
Weather type	F		Meteo appendix
Wind direction	350	degrees	Meteo appendix
Pumped inflow	200	kg/s	Assumption
Fracture length	9.1	m	Aerial imagery report, figure 5: 28-33 feet.
Relative size	1		
Depth	1.5	m	Materials lab factual report: 40 inch
Soil type	Sand		Report, Table 4: “shale”

10.2 Discussion of alternative dose relationships

In Section 5.4 three alternative dose relationships were identified. These alternatives will be evaluated in this section.

1. $B = 1.5, C = 5\ kW/m^2$, and 50%
2. $B = 1.5, C = 8\ kW/m^2$, and 10%
3. $B = 2.5, C = 5\ kW/m^2$, and 10%

Figure 28 shows the proposed dose relationship and the three alternatives. Table 19 shows the results of the evaluation described in

the appendix in Chapter 9. Table 20 shows the time to ignition for a range of heat fluxes.

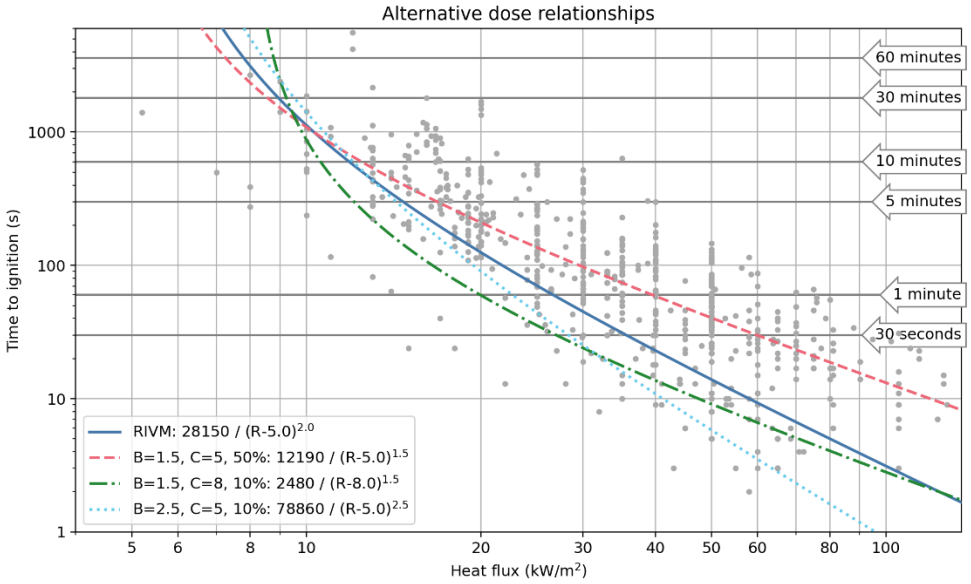

Figure 28 The proposed dose relationship and three alternatives

The first alternative (B=1.5, C=5 kW/m^2, 50%) has a very high N ratio in Table 19. It calculates much longer times to ignition for higher heat fluxes, as can be seen in Figure 28 and Table 20.

The evaluation of the second alternative (B=1.5, C=8 kW/m^2, 10%) shows the N ratio is the same as for the proposal and the RMS and RMS ratio are lower. Table 20 shows that for fluxes above 9 to 10 kW/m^2 the time to ignition is actually much shorter compared to the other options. Compared to the proposal and the two other alternatives, it is also the one that overestimates the distance to the damage the most (Table 4).

The evaluation of the third alternative (B=2.5, C=5 kW/m^2, 10%) shows a high RMS ratio and a low N ratio (see the discussion in Section 9.2).

Table 19 Results of the evaluation for the proposed dose relationship (left) and three alternatives

B **C** **Percentile**	**2** **5** **20%**	**1.5** **5** **50%**	**1.5** **8** **10%**	**2.5** **5** **10%**
A	28150	12190	2480	78860
N <20.0	38	66	19	34
N >=20.0	83	237	42	27
N ratio	2.2	3.6	2.2	1.3
RMS <20.0	0.647	0.465	0.4	0.816
RMS >=20.0	0.31	0.439	0.246	0.223
RMS ratio	2.1	1.1	1.6	3.7
RMS all	0.445	0.445	0.292	0.627

Table 20 Time to ignition for the proposed dose relationship (left) and three alternatives

B **C** **Percentile**	**2** **5** **20%**	**1.5** **5** **50%**	**1.5** **8** **10%**	**2.5** **5** **10%**
6	7h 49m	3h 23m	-	21h 54m
9	29m 19s	25m 24s	41m 20s	41m 4s
10	18m 46s	18m 10s	14m 37s	23m 31s
15	4m 42s	6m 25s	2m 14s	4m 9s
20	2m 5s	3m 30s	60s	1m 30s
30	45s	1m 38s	24s	25s
35	31s	1m 14s	18s	16s
50	14s	40s	9s	6s

11 Experimental data

11.1 Data sources

Table 21 Sources of the experimental data. When the data was taken from the HSE report [8], not the article itself, this is denoted by (HSE). An asterisk (*) indicates the paper itself was not studied.

Short name	Reference	Short description
An, 2015	[13]	Two types of polystyrene with different thicknesses are compared.
Bell, 1995 (HSE)	?	No reference found.
Bilbao, 2001	[36]	The effect of air current over the samples was studied. Only data with no air current was used for the analysis.
Bilbao, 2002 (HSE)	[21]	Measurements with constant and variable heat flux. Only data with constant heat flux was used.
Chen, 2016	[37]	Study of the correlation of different parameters measured in an experiment.
Delichatsios, 2003 (HSE)	[38]	Experimental paper to validate theoretical model.
Delichatsios, 2005	[39]	Study of the effect of different percentages oxygen in the air. Only data with 21 v% oxygen was used in the analysis.
Gibson, 1995 (HSE)	[40]*	
Hallman, 1972 (HSE)	[41]*	
Hilado, 1998 (HSE)	[42]*	Book "Flammability Handbook for Plastics"
Lawson, 1952 (HSE)	[20]*	
Luzik, 1988 (HSE)	[43]*	Results of a study into the cause of the explosion at Pepco, Nevada.
Moghtaderi, 1997 (HSE)	[14]	Experimental study to support the development of a theoretical model.
Moysey, 1968 (HSE)	[25]*	
Panagiotou, 2004	[12]	PhD thesis on the methodology of ignition experiments.
Safronava, 2015	[18]	Study of the effect of moisture content on the time to ignition of plastics.
Shields, 1995 (HSE)	[19][18]	Experimental study to support the development of a theoretical model.
Spearpoint, 2001	[17]	Study of the important variables in determining the time to ignition.
Staggs, 2003 (HSE)	[24]	Study of the effect of paint on the time to ignition.
Thomson, 1987 (HSE)	[44]*	
Thomson, 1989 (HSE)	[45]*	

[18] The reference in the HSE report says Shields & Silcock, but this should probably be Silcock & Shields. The journal, name of the article, and the volume correspond with the reference in the HSE report.

Short name	Reference	Short description
Vermesi, 2016	[11]	Measurements with constant and variable heat flux. Only data with constant heat flux was used.
Wesson, 1971 (HSE)	[46]*	
Yang, 2003 (HSE)	[47]	Study of pyrolysis of charred wood.
Zhang, 2018	[15]	Study into the effect of flame retardant on polycarbonaat

11.2 Data

The table on the next pages shows all data used in this report.
Explanation of the columns:

- Class: the classes used in the figures in this paper, for example 'plastic' and 'wood'.
- Material group: groups of materials. The material class 'PS' for example covers both extruded and expanded PS.
- Material: the material name, as defined in the papers.
- Details: details as given in the papers.
- Heat flux: in kW/m^2
- Time to ignition: in seconds
- Reference: using the naming convention in Table 21

Class	Material group	Material	Details	Heat flux [kW/m^2]	Time to ignition [s]	Reference
Plastic	PS	Extruded PS	2 cm thick	25	129	An et al., 2015
		Extruded PS	3 cm thick	25	140	An et al., 2015
		Extruded PS	2 cm thick	35	39	An et al., 2015
		Extruded PS	3 cm thick	35	44	An et al., 2015
		Extruded PS	4 cm thick	35	50	An et al., 2015
		Extruded PS	5 cm thick	35	62	An et al., 2015
		Extruded PS	2 cm thick	45	22	An et al., 2015
		Extruded PS	3 cm thick	45	23.5	An et al., 2015
		Extruded PS	4 cm thick	45	28	An et al., 2015
		Extruded PS	5 cm thick	45	33	An et al., 2015
		Expanded PS	2 cm thick	25	237	An et al., 2015
		Expanded PS	3 cm thick	25	256	An et al., 2015
		Expanded PS	2 cm thick	35	54	An et al., 2015
		Expanded PS	3 cm thick	35	60	An et al., 2015
		Expanded PS	4 cm thick	35	59	An et al., 2015
		Expanded PS	5 cm thick	35	86	An et al., 2015
		Expanded PS	2 cm thick	45	33	An et al., 2015
		Expanded PS	3 cm thick	45	36.5	An et al., 2015
		Expanded PS	4 cm thick	45	39	An et al., 2015
		Expanded PS	5 cm thick	45	46	An et al., 2015
		PS		15.5	365	Thomson et al., 1987
		PS		19	236	Thomson et al., 1987
		PS		28	102	Thomson et al., 1987
		PS		34	67	Thomson et al., 1987
		PS	Fire Retarded	25	268	Thomson et al., 1989
		PS	Fire Retarded	25	291	Thomson et al., 1989
		PS	Fire Retarded	33	124	Thomson et al., 1989
		PS	Fire Retarded	33	124	Thomson et al., 1989

Class	Material group	Material	Details	Heat flux [kW/m^2]	Time to ignition [s]	Reference
		PS		13	496	Thomson et al., 1989
		PS		13	610	Thomson et al., 1989
		PS		19	183	Thomson et al., 1989
		PS		19	209	Thomson et al., 1989
		PS		25	110	Thomson et al., 1989
		PS		25	120	Thomson et al., 1989
		PS		33	74	Thomson et al., 1989
		PS		33	74	Thomson et al., 1989
Plastic	Rubber	EPDM		25	488	Chen et al., 2016
		EPDM		30	202	Chen et al., 2016
		EPDM		35	158	Chen et al., 2016
		EPDM		40	110	Chen et al., 2016
		EPDM		45	77	Chen et al., 2016
		EPDM		50	58	Chen et al., 2016
		EPDM		55	42	Chen et al., 2016
		EPDM		60	40	Chen et al., 2016
		EPDM		65	38	Chen et al., 2016
Plastic	PMMA	PMMA		20	520	Vermesi et al., 2016
		PMMA	Black Benzene	37.3	93	Hallman, 1972
		PMMA	Black Benzene	37.3	100	Hallman, 1972
		PMMA	Black Benzene	52.7	40	Hallman, 1972
		PMMA	Black Benzene	63.8	26	Hallman, 1972
		PMMA	Black Benzene	80.4	17	Hallman, 1972
		PMMA	Black Benzene	90.2	14	Hallman, 1972
		PMMA	Black Benzene	105.1	9	Hallman, 1972
		PMMA	Black Benzene	122.6	7	Hallman, 1972
		PMMA	Clear Benzene	28.5	224	Hallman, 1972
		PMMA	Clear Benzene	38.8	104	Hallman, 1972
		PMMA	Clear Benzene	50.7	66	Hallman, 1972

Class	Material group	Material	Details	Heat flux [kW/m^2]	Time to ignition [s]	Reference
		PMMA	Clear Benzene	63.8	28	Hallman, 1972
		PMMA	Clear Benzene	77.3	24	Hallman, 1972
		PMMA	Clear Benzene	90.2	19	Hallman, 1972
		PMMA	Clear Benzene	105.1	16	Hallman, 1972
		PMMA	Clear Benzene	127.4	9	Hallman, 1972
		PMMA	1/8 inch	58	115	Hilado, 1998
		PMMA	1/8 inch	81	33	Hilado, 1998
		PMMA	1/8 inch	105	31	Hilado, 1998
		PMMA	Finnacryl	13	1125	Thomson et al., 1987
		PMMA	Finnacryl	13	328	Thomson et al., 1989
		PMMA	Finnacryl	13	280	Thomson et al., 1989
		PMMA	Finnacryl	15	391	Thomson et al., 1987
		PMMA	Finnacryl	18.5	227	Thomson et al., 1987
		PMMA	Finnacryl	19	167	Thomson et al., 1989
		PMMA	Finnacryl	19	150	Thomson et al., 1989
		PMMA	Finnacryl	22	148	Thomson et al., 1987
		PMMA	Finnacryl	25	84	Thomson et al., 1989
		PMMA	Finnacryl	25	80	Thomson et al., 1989
		PMMA	Finnacryl	25.5	99	Thomson et al., 1987
		PMMA	Finnacryl	29	80	Thomson et al., 1987
		PMMA	Finnacryl	33	42	Thomson et al., 1989
		PMMA	Finnacryl	33	42	Thomson et al., 1989
		PMMA	Finnacryl	38	24	Thomson et al., 1987
		PMMA	Fire Retarded	19	352	Thomson et al., 1989
		PMMA	Fire Retarded	19	281	Thomson et al., 1989
		PMMA	Fire Retarded	25	194	Thomson et al., 1989
		PMMA	Fire Retarded	25	184	Thomson et al., 1989
		PMMA	Fire Retarded	33	89	Thomson et al., 1989
		PMMA	Fire Retarded	33	89	Thomson et al., 1989

Class	Material group	Material	Details	Heat flux [kW/m^2]	Time to ignition [s]	Reference
		PMMA	Perspex	13	287	Thomson et al., 1989
		PMMA	Perspex	13	223	Thomson et al., 1989
		PMMA	Perspex	14	461	Thomson et al., 1987
		PMMA	Perspex	17	288	Thomson et al., 1987
		PMMA	Perspex	19	127	Thomson et al., 1989
		PMMA	Perspex	19	109	Thomson et al., 1989
		PMMA	Perspex	20.5	173	Thomson et al., 1987
		PMMA	Perspex	24	115	Thomson et al., 1987
		PMMA	Perspex	25	58	Thomson et al., 1989
		PMMA	Perspex	25	52	Thomson et al., 1989
		PMMA	Perspex	30	67	Thomson et al., 1987
		PMMA	Perspex	33	30	Thomson et al., 1989
		PMMA	Perspex	33	30	Thomson et al., 1989
		PMMA	Perspex	37.5	39	Thomson et al., 1987
		PMMA		10	1427	Panagiotou, 2004
		PMMA		11	933	Panagiotou, 2004
		PMMA		13	637	Panagiotou, 2004
		PMMA		14.8	461	Panagiotou, 2004
		PMMA		17	285	Panagiotou, 2004
		PMMA		17	264	Panagiotou, 2004
		PMMA		19	245	Panagiotou, 2004
		PMMA		19	278	Panagiotou, 2004
		PMMA		30	115	Panagiotou, 2004
		PMMA		40	58	Panagiotou, 2004
		PMMA		50	45	Panagiotou, 2004
		PMMA		60	24	Panagiotou, 2004
		PMMA	2.4% moisture	10	532	Safronava et al., 2014
		PMMA	2.4% moisture	15	212	Safronava et al., 2014
		PMMA	2.4% moisture	20	150	Safronava et al., 2014

Class	Material group	Material	Details	Heat flux [kW/m^2]	Time to ignition [s]	Reference
		PMMA	2.4% moisture	30	72	Safronava et al., 2014
		PMMA	2.4% moisture	50	33	Safronava et al., 2014
		PMMA	2.4% moisture	75	17	Safronava et al., 2014
		PMMA	0.4% moisture	10	504	Safronava et al., 2014
		PMMA	0.4% moisture	15	199	Safronava et al., 2014
		PMMA	0.4% moisture	20	115	Safronava et al., 2014
		PMMA	0.4% moisture	30	53	Safronava et al., 2014
		PMMA	0.4% moisture	50	24	Safronava et al., 2014
		PMMA	0.4% moisture	75	17	Safronava et al., 2014
		PMMA	0% moisture	10	1053	Safronava et al., 2014
		PMMA	0% moisture	15	346	Safronava et al., 2014
		PMMA	0% moisture	20	243	Safronava et al., 2014
		PMMA	0% moisture	30	82	Safronava et al., 2014
		PMMA	0% moisture	50	36	Safronava et al., 2014
		PMMA	0% moisture	75	20	Safronava et al., 2014
Plastic	PC	Flame retardant PC		25	574	Zhang et al., 2018
		Flame retardant PC		30	443	Zhang et al., 2018
		Flame retardant PC		35	101	Zhang et al., 2018
		Flame retardant PC		40	45	Zhang et al., 2018
		Flame retardant PC		45	33	Zhang et al., 2018
		Flame retardant PC		50	26	Zhang et al., 2018
		Flame retardant PC		55	23	Zhang et al., 2018
		Flame retardant PC		60	11	Zhang et al., 2018
		PC	Fire Retarded	25	267	Hilado, 1998
		PC	Fire Retarded	50	53	Hilado, 1998
		PC	Fire Retarded	75	28	Hilado, 1998
		PC	Non Fire Retarded	25	189	Hilado, 1998
		PC	Non Fire Retarded	50	49	Hilado, 1998
		PC	Non Fire Retarded	75	21	Hilado, 1998

Class	Material group	Material	Details	Heat flux [kW/m^2]	Time to ignition [s]	Reference
		PC		30	300	Panagiotou, 2004
		PC		40	177	Panagiotou, 2004
		PC		50	125	Panagiotou, 2004
		PC		60	70	Panagiotou, 2004
		PC	0.6% moisture	25	524	Safronava et al., 2014
		PC	0.6% moisture	30	249	Safronava et al., 2014
		PC	0.6% moisture	40	128	Safronava et al., 2014
		PC	0.6% moisture	50	70	Safronava et al., 2014
		PC	0.6% moisture	70	25	Safronava et al., 2014
		PC	0.2% moisture	25	476	Safronava et al., 2014
		PC	0.2% moisture	30	181	Safronava et al., 2014
		PC	0.2% moisture	40	124	Safronava et al., 2014
		PC	0.2% moisture	50	62	Safronava et al., 2014
		PC	0.2% moisture	70	31	Safronava et al., 2014
		PC	0% moisture	25	491	Safronava et al., 2014
		PC	0% moisture	30	350	Safronava et al., 2014
		PC	0% moisture	40	162	Safronava et al., 2014
		PC	0% moisture	50	105	Safronava et al., 2014
		PC	0% moisture	70	49	Safronava et al., 2014
Plastic	Acrylic	Acrylic	Carpet	58	38	Hilado, 1998
		Acrylic	Carpet	81	15	Hilado, 1998
		Acrylic	Carpet	105	9	Hilado, 1998
Plastic	Nylon	Nylon	Carpet	58	29	Hilado, 1998
		Nylon	Carpet	81	17	Hilado, 1998
		Nylon	Carpet	105	13	Hilado, 1998
		Nylon	Clothing	58	22	Hilado, 1998
		Nylon	Clothing	81	26	Hilado, 1998
		Nylon	Clothing	105	7	Hilado, 1998
		Nylon		19	628	Panagiotou, 2004

Class	Material group	Material	Details	Heat flux [kW/m^2]	Time to ignition [s]	Reference
		Nylon		30	372	Panagiotou, 2004
		Nylon		40	140	Panagiotou, 2004
		Nylon		50	86	Panagiotou, 2004
		Nylon		60	51	Panagiotou, 2004
Plastic	Epoxy	Epoxy		30	100	Gibson, 1995
		Epoxy		40	90	Gibson, 1995
		Epoxy		50	50	Gibson, 1995
		Epoxy		60	33	Gibson, 1995
		Epoxy		80	17	Gibson, 1995
Plastic	Resin	Phenolic resin	40% glass	35	638	Bell, 1995
		Phenolic resin	40% glass	50	147	Bell, 1995
		Phenolic resin	40% glass	75	66	Bell, 1995
		Phenolic resin	65% glass	50	132	Bell, 1995
		Phenolic resin	65% glass	75	46	Bell, 1995
		Phenolic resin		30	450	Gibson, 1995
		Phenolic resin		40	300	Gibson, 1995
		Phenolic resin		50	110	Gibson, 1995
		Phenolic resin		60	87	Gibson, 1995
		Phenolic resin		80	55	Gibson, 1995
Plastic	PE	PE		30	90	Gibson, 1995
		PE		40	65	Gibson, 1995
		PE		50	30	Gibson, 1995
		PE		60	23	Gibson, 1995
		PE		80	14	Gibson, 1995
		PE		19	524	Thomson et al., 1987
		PE		23	315	Thomson et al., 1987
		PE		27	223	Thomson et al., 1987
		PE		28.5	172	Thomson et al., 1987
		PE		34	83	Thomson et al., 1987

Class	Material group	Material	Details	Heat flux [kW/m^2]	Time to ignition [s]	Reference
		PE		25	141	Thomson et al., 1989
		PE		25	172	Thomson et al., 1989
		PE		33	90	Thomson et al., 1989
		PE		33	90	Thomson et al., 1989
Plastic	POM	POM		15.5	714	Thomson et al., 1987
		POM		17	386	Thomson et al., 1987
		POM		21	248	Thomson et al., 1987
		POM		25	184	Thomson et al., 1987
		POM		28	138	Thomson et al., 1987
		POM		34	79	Thomson et al., 1987
		POM		13	428	Thomson et al., 1989
		POM		13	573	Thomson et al., 1989
		POM		19	227	Thomson et al., 1989
		POM		19	275	Thomson et al., 1989
		POM		25	122	Thomson et al., 1989
		POM		25	143	Thomson et al., 1989
		POM		33	84	Thomson et al., 1989
		POM		33	84	Thomson et al., 1989
		POM		10	1877	Panagiotou, 2004
		POM		11	1081	Panagiotou, 2004
		POM		13	770	Panagiotou, 2004
		POM		14.8	668	Panagiotou, 2004
		POM		17	308	Panagiotou, 2004
		POM		19	210	Panagiotou, 2004
		POM		30	105	Panagiotou, 2004
		POM		40	63	Panagiotou, 2004
		POM		50	37	Panagiotou, 2004
		POM		60	32	Panagiotou, 2004
		POM	1.7% moisture	10	686	Safronava et al., 2014

Class	Material group	Material	Details	Heat flux [kW/m^2]	Time to ignition [s]	Reference
		POM	1.7% moisture	20	120	Safronava et al., 2014
		POM	1.7% moisture	40	38	Safronava et al., 2014
		POM	1.7% moisture	50	26	Safronava et al., 2014
		POM	1.7% moisture	70	14	Safronava et al., 2014
		POM	0.3% moisture	10	853	Safronava et al., 2014
		POM	0.3% moisture	20	203	Safronava et al., 2014
		POM	0.3% moisture	40	65	Safronava et al., 2014
		POM	0.3% moisture	50	39	Safronava et al., 2014
		POM	0.3% moisture	70	20	Safronava et al., 2014
		POM	0% moisture	10	532	Safronava et al., 2014
		POM	0% moisture	20	200	Safronava et al., 2014
		POM	0% moisture	40	61	Safronava et al., 2014
		POM	0% moisture	50	39	Safronava et al., 2014
		POM	0% moisture	70	22	Safronava et al., 2014
Plastic	PP	PP		17	372	Thomson et al., 1987
		PP		21	230	Thomson et al., 1987
		PP		25	139	Thomson et al., 1987
		PP		31	86	Thomson et al., 1987
		PP		42.5	46	Thomson et al., 1987
		PP	Fire Retarded	25	269	Thomson et al., 1989
		PP	Fire Retarded	25	285	Thomson et al., 1989
		PP	Fire Retarded	33	90	Thomson et al., 1989
		PP	Fire Retarded	33	90	Thomson et al., 1989
		PP		13	302	Thomson et al., 1989
		PP		13	442	Thomson et al., 1989
		PP		19	146	Thomson et al., 1989
		PP		19	172	Thomson et al., 1989
		PP		25	75	Thomson et al., 1989
		PP		25	91	Thomson et al., 1989

Class	Material group	Material	Details	Heat flux [kW/m^2]	Time to ignition [s]	Reference
		PP		33	57	Thomson et al., 1989
		PP		33	57	Thomson et al., 1989
Plastic	Vinyl Ester	Vinyl Ester		30	63	Gibson, 1995
		Vinyl Ester		40	44	Gibson, 1995
		Vinyl Ester		50	22	Gibson, 1995
		Vinyl Ester		60	18	Gibson, 1995
		Vinyl Ester		80	10	Gibson, 1995
Plastic	PVC	PVC	Extruded Grey 3mm	15	655	Shields, 1995
		PVC	Extruded Grey 3mm	20	184	Shields, 1995
		PVC	Extruded Grey 3mm	30	71	Shields, 1995
		PVC	Extruded Grey 3mm	40	43	Shields, 1995
		PVC	Extruded Grey 3mm	50	26	Shields, 1995
		PVC	Compressed White 5mm	15	653	Shields, 1995
		PVC	Compressed White 5mm	20	332	Shields, 1995
		PVC	Compressed White 5mm	30	209	Shields, 1995
		PVC	Compressed White 5mm	40	95	Shields, 1995
		PVC	Compressed White 5mm	50	55	Shields, 1995
		PVC		21.3	690	Panagiotou, 2004
		PVC		23.7	480	Panagiotou, 2004
		PVC		26	300	Panagiotou, 2004
		PVC		30	140	Panagiotou, 2004
		PVC		40	65	Panagiotou, 2004
		PVC		50	40	Panagiotou, 2004
		PVC		60	30	Panagiotou, 2004
Plastic	HIPS	HIPS		17	510	Panagiotou, 2004
		HIPS		19	350	Panagiotou, 2004
		HIPS		30	120	Panagiotou, 2004
		HIPS		40	63	Panagiotou, 2004
		HIPS		50	48	Panagiotou, 2004

Class	Material group	Material	Details	Heat flux [kW/m^2]	Time to ignition [s]	Reference
		HIPS		60	28	Panagiotou, 2004
Plastic	ABS	ABS		13	728	Panagiotou, 2004
		ABS		14.8	544	Panagiotou, 2004
		ABS		17	292	Panagiotou, 2004
		ABS		19	208	Panagiotou, 2004
		ABS		30	75	Panagiotou, 2004
		ABS		40	46	Panagiotou, 2004
		ABS		50	34	Panagiotou, 2004
		ABS		60	26	Panagiotou, 2004
Plastic	HDPE	HDPE		17	907	Panagiotou, 2004
		HDPE		19	482	Panagiotou, 2004
		HDPE		30	157	Panagiotou, 2004
		HDPE		40	83	Panagiotou, 2004
		HDPE		50	71	Panagiotou, 2004
Plastic	PA66	PA66	9.2% moisture	15	792	Safronava et al., 2014
		PA66	9.2% moisture	20	445	Safronava et al., 2014
		PA66	9.2% moisture	30	190	Safronava et al., 2014
		PA66	9.2% moisture	40	130	Safronava et al., 2014
		PA66	9.2% moisture	50	78	Safronava et al., 2014
		PA66	9.2% moisture	70	37	Safronava et al., 2014
		PA66	2.6% moisture	15	440	Safronava et al., 2014
		PA66	2.6% moisture	20	224	Safronava et al., 2014
		PA66	2.6% moisture	30	127	Safronava et al., 2014
		PA66	2.6% moisture	40	91	Safronava et al., 2014
		PA66	2.6% moisture	50	58	Safronava et al., 2014
		PA66	2.6% moisture	70	27	Safronava et al., 2014
		PA66	0% moisture	15	631	Safronava et al., 2014
		PA66	0% moisture	20	502	Safronava et al., 2014
		PA66	0% moisture	30	205	Safronava et al., 2014

Class	Material group	Material	Details	Heat flux [kW/m^2]	Time to ignition [s]	Reference
		PA66	0% moisture	40	120	Safronava et al., 2014
		PA66	0% moisture	50	74	Safronava et al., 2014
		PA66	0% moisture	70	35	Safronava et al., 2014
Plastic	PPSU	PPSU	1.4% moisture	30	421	Safronava et al., 2014
		PPSU	1.4% moisture	40	107	Safronava et al., 2014
		PPSU	1.4% moisture	50	50	Safronava et al., 2014
		PPSU	1.4% moisture	70	17	Safronava et al., 2014
		PPSU	0.6% moisture	30	420	Safronava et al., 2014
		PPSU	0.6% moisture	40	105	Safronava et al., 2014
		PPSU	0.6% moisture	50	50	Safronava et al., 2014
		PPSU	0.6% moisture	70	20	Safronava et al., 2014
		PPSU	0% moisture	30	520	Safronava et al., 2014
		PPSU	0% moisture	40	201	Safronava et al., 2014
		PPSU	0% moisture	50	115	Safronava et al., 2014
		PPSU	0% moisture	70	63	Safronava et al., 2014
Wood	Pine	Maritime pine	9 wt% moisture	14.3	389	Bilbao et al., 2001
		Maritime pine	9 wt% moisture	20	180	Bilbao et al., 2001
		Maritime pine	9 wt% moisture	25.8	36	Bilbao et al., 2001
		Maritime pine	9 wt% moisture	29.9	29	Bilbao et al., 2001
		Maritime pine	9 wt% moisture	44.1	13	Bilbao et al., 2001
		Maritime pine	9 wt% moisture	53.5	10	Bilbao et al., 2001
		Redwood	Along grain, 8.6% moist.	13	2170	Spearpoint et al., 2001
		Redwood	Across grain, 7.4% moist.	9	1416	Spearpoint et al., 2001
		Douglas fir	Along grain, 7.4% moist.	12	5580	Spearpoint et al., 2001
		Douglas fir	Across grain, 8.5% moist.	9	2395	Spearpoint et al., 2001
		Douglas Fir		15.9	1179	Moysey et al., 1968
		Douglas Fir		16.7	696	Moysey et al., 1968
		Douglas Fir		17.4	385	Moysey et al., 1968
		Douglas Fir		18.8	327	Moysey et al., 1968

Class	Material group	Material	Details	Heat flux [kW/m^2]	Time to ignition [s]	Reference
		Douglas Fir		19.6	268	Moysey et al., 1968
		Douglas Fir		20.6	220	Moysey et al., 1968
		Douglas Fir		21.6	158	Moysey et al., 1968
		Douglas Fir	3/4 inch	58	46	Hilado, 1998
		Douglas Fir	3/4 inch	81	23	Hilado, 1998
		Douglas Fir	3/4 inch	105	11	Hilado, 1998
		Pine Radiata	0% moisture	20	179	Moghtaderi, 1997
		Pine Radiata	0% moisture	30	19	Moghtaderi, 1997
		Pine Radiata	0% moisture	40	9	Moghtaderi, 1997
		Pine Radiata	0% moisture	50	5	Moghtaderi, 1997
		Pine Radiata	0% moisture	60	3	Moghtaderi, 1997
		Pine Radiata	15% moisture	20	295	Moghtaderi, 1997
		Pine Radiata	15% moisture	30	52	Moghtaderi, 1997
		Pine Radiata	15% moisture	40	18	Moghtaderi, 1997
		Pine Radiata	15% moisture	50	11	Moghtaderi, 1997
		Pine Radiata	15% moisture	60	7	Moghtaderi, 1997
		Pine Radiata	22% moisture	20	420	Moghtaderi, 1997
		Pine Radiata	22% moisture	30	67	Moghtaderi, 1997
		Pine Radiata	22% moisture	40	30	Moghtaderi, 1997
		Pine Radiata	22% moisture	50	11	Moghtaderi, 1997
		Pine Radiata	22% moisture	60	9	Moghtaderi, 1997
		Pine Radiata	30% moisture	20	540	Moghtaderi, 1997
		Pine Radiata	30% moisture	30	93	Moghtaderi, 1997
		Pine Radiata	30% moisture	40	36	Moghtaderi, 1997
		Pine Radiata	30% moisture	50	19	Moghtaderi, 1997
		Pine Radiata	30% moisture	60	11	Moghtaderi, 1997
		Pine Sugar	10% moisture	20	150	Moghtaderi, 1997
		Pine Sugar	10% moisture	25	49	Moghtaderi, 1997
		Pine Sugar	10% moisture	35	13	Moghtaderi, 1997

Class	Material group	Material	Details	Heat flux [kW/m^2]	Time to ignition [s]	Reference
		Pine Sugar	10% moisture	45	6	Moghtaderi, 1997
		Pine Sugar	10% moisture	55	3	Moghtaderi, 1997
		Pine		14	450	Bilbao, 2002
		Pine		14	500	Bilbao, 2002
		Pine		15	24	Bilbao, 2002
		Pine		26	32	Bilbao, 2002
		Pine		30	30	Bilbao, 2002
		Pine		31	22	Bilbao, 2002
		Pine		41	9	Bilbao, 2002
		Pine		41	13	Bilbao, 2002
		Pine		44	13	Bilbao, 2002
		Pine		44	14	Bilbao, 2002
		Pine		53	9	Bilbao, 2002
		Pine		53	10	Bilbao, 2002
		Pine		58	7	Bilbao, 2002
		Pine Radiata		20	484	Delichatsios, 2003
		Pine Radiata		25	153	Delichatsios, 2003
		Pine Radiata		30	132	Delichatsios, 2003
		Pine Radiata		45	30	Delichatsios, 2003
		Pine Radiata		50	22	Delichatsios, 2003
		Whitewood	3/4 inch	20.4	213	Lawson et al., 1952
		Whitewood	3/4 inch	24	78	Lawson et al., 1952
		Whitewood	3/4 inch	25.2	43	Lawson et al., 1952
		Whitewood	3/4 inch	28.8	33	Lawson et al., 1952
		Whitewood	3/4 inch	32.4	20	Lawson et al., 1952
		Whitewood	3/4 inch	39.6	15	Lawson et al., 1952
		Whitewood	3/4 inch	54	9	Lawson et al., 1952
		Whitewood	3/4 inch	70.8	4	Lawson et al., 1952
Wood	Maple	Maple	Along grain, 4.8% moist.	12	4200	Spearpoint et al., 2001

Class	Material group	Material	Details	Heat flux [kW/m^2]	Time to ignition [s]	Reference
		Maple	Across grain, 4.8% moist.	8	2680	Spearpoint et al., 2001
		Maple	10% moisture	14	960	Moghtaderi, 1997
		Maple	10% moisture	18	160	Moghtaderi, 1997
		Maple	10% moisture	20	150	Moghtaderi, 1997
		Maple	10% moisture	25	69	Moghtaderi, 1997
		Maple	10% moisture	37	20	Moghtaderi, 1997
		Maple	10% moisture	50	8	Moghtaderi, 1997
		Maple	10% moisture	65	5	Moghtaderi, 1997
Wood	Beech	Beech		20	1489	Yang, 2003
		Beech		30	159	Yang, 2003
		Beech		40	79	Yang, 2003
		Beech		50	49	Yang, 2003
Wood	Cedar	Cedar	3/4 inch	17	125	Lawson et al., 1952
		Cedar	3/4 inch	22	57	Lawson et al., 1952
		Cedar	3/4 inch	24	36	Lawson et al., 1952
		Cedar	3/4 inch	27	23	Lawson et al., 1952
		Cedar	3/4 inch	28	13	Lawson et al., 1952
		Cedar	3/4 inch	45	6	Lawson et al., 1952
		Cedar	3/4 inch	60	4	Lawson et al., 1952
		Cedar	Unweathered	15.5	968	Moysey et al., 1968
		Cedar	Unweathered	16.1	800	Moysey et al., 1968
		Cedar	Unweathered	16.7	600	Moysey et al., 1968
		Cedar	Unweathered	17.4	327	Moysey et al., 1968
		Cedar	Unweathered	19	148	Moysey et al., 1968
		Cedar	Unweathered	19.8	139	Moysey et al., 1968
		Cedar	Unweathered	20.9	94	Moysey et al., 1968
		Cedar	Weathered	16.1	1068	Moysey et al., 1968
		Cedar	Weathered	16.4	936	Moysey et al., 1968
		Cedar	Weathered	16.7	744	Moysey et al., 1968

Class	Material group	Material	Details	Heat flux [kW/m^2]	Time to ignition [s]	Reference
		Cedar	Weathered	17.4	454	Moysey et al., 1968
		Cedar	Weathered	18.2	398	Moysey et al., 1968
		Cedar	Weathered	19.8	327	Moysey et al., 1968
Wood	Cherry	Cherry		20	1611	Yang, 2003
		Cherry		30	193	Yang, 2003
		Cherry		40	83	Yang, 2003
		Cherry		50	49	Yang, 2003
Wood	Hard wood	Freijo	3/4 inch	20.7	425	Lawson et al., 1952
		Freijo	3/4 inch	26.4	67	Lawson et al., 1952
		Freijo	3/4 inch	28.8	43	Lawson et al., 1952
		Freijo	3/4 inch	33.6	32	Lawson et al., 1952
		Freijo	3/4 inch	39.6	23	Lawson et al., 1952
		Freijo	3/4 inch	46.8	13	Lawson et al., 1952
		Freijo	3/4 inch	54	12	Lawson et al., 1952
		Freijo	3/4 inch	68.4	5	Lawson et al., 1952
		Iroko	3/4 inch	24.2	375	Lawson et al., 1952
		Iroko	3/4 inch	27.6	86	Lawson et al., 1952
		Iroko	3/4 inch	30	57	Lawson et al., 1952
		Iroko	3/4 inch	39.6	30	Lawson et al., 1952
		Iroko	3/4 inch	48	25	Lawson et al., 1952
		Iroko	3/4 inch	54	20	Lawson et al., 1952
		Iroko	3/4 inch	63.6	12	Lawson et al., 1952
		Kampas		20	1699	Yang, 2003
		Kampas		30	443	Yang, 2003
		Kampas		40	134	Yang, 2003
		Kampas		50	79	Yang, 2003
		Mahogany	3/4 inch	16.8	359	Lawson et al., 1952
		Mahogany	3/4 inch	20.4	241	Lawson et al., 1952
		Mahogany	3/4 inch	24	93	Lawson et al., 1952

Class	Material group	Material	Details	Heat flux [kW/m^2]	Time to ignition [s]	Reference
		Mahogany	3/4 inch	26.4	64	Lawson et al., 1952
		Mahogany	3/4 inch	34.8	31	Lawson et al., 1952
		Mahogany	3/4 inch	39.6	18	Lawson et al., 1952
		Mahogany	3/4 inch	63.6	6	Lawson et al., 1952
		Mahogany	3/4 inch	72	4	Lawson et al., 1952
Wood	Oak	Oak	3/4 inch	23.4	241	Lawson et al., 1952
		Oak	3/4 inch	26.4	93	Lawson et al., 1952
		Oak	3/4 inch	39.6	24	Lawson et al., 1952
		Oak	3/4 inch	46.8	17	Lawson et al., 1952
		Oak	3/4 inch	50.4	13	Lawson et al., 1952
		Oak	3/4 inch	68.4	6	Lawson et al., 1952
		Oak	Oven dried	38.8	305	Wesson et al., 1971
		Oak	Oven dried	56.3	96	Wesson et al., 1971
		Oak	Oven dried	58.5	86	Wesson et al., 1971
		Oak	Oven dried	75.8	53	Wesson et al., 1971
		Oak	Oven dried	75.8	57	Wesson et al., 1971
		Oak	Oven dried	78.7	40	Wesson et al., 1971
		Oak	Oven dried	87.9	34	Wesson et al., 1971
		Oak	Oven dried	94.8	28	Wesson et al., 1971
		Oak	Oven dried	102	27	Wesson et al., 1971
		Oak	Oven dried	109.9	24	Wesson et al., 1971
		Oak	Oven dried	114.1	20	Wesson et al., 1971
		Oak	Oven dried	114.1	23	Wesson et al., 1971
		Oak	Oven dried	125.6	13	Wesson et al., 1971
		Oak	Oven dried	125.6	15	Wesson et al., 1971
		Oak		20	1348	Yang, 2003
		Oak		30	214	Yang, 2003
		Oak		40	111	Yang, 2003
		Oak		50	61	Yang, 2003

Class	Material group	Material	Details	Heat flux [kW/m^2]	Time to ignition [s]	Reference
Proc. wood	Plywood	Plywood		25	124	Delichatsios, 2005
		Plywood		35	106	Delichatsios, 2005
		Plywood		50	118	Delichatsios, 2005
Proc. wood	Fibre ins. board	Fibre insulation board	1/2 inch	5.2	1410	Lawson et al., 1952
		Fibre insulation board	1/2 inch	7	500	Lawson et al., 1952
		Fibre insulation board	1/2 inch	8	388	Lawson et al., 1952
		Fibre insulation board	1/2 inch	8	275	Lawson et al., 1952
		Fibre insulation board	1/2 inch	10	238	Lawson et al., 1952
		Fibre insulation board	1/2 inch	11	116	Lawson et al., 1952
		Fibre insulation board	1/2 inch	13	82	Lawson et al., 1952
		Fibre insulation board	1/2 inch	14	64	Lawson et al., 1952
		Fibre insulation board	1/2 inch	17	40	Lawson et al., 1952
		Fibre insulation board	1/2 inch	18	24	Lawson et al., 1952
		Fibre insulation board	1/2 inch	22	13	Lawson et al., 1952
		Fibre insulation board	1/2 inch	32	8	Lawson et al., 1952
		Fibre insulation board	1/2 inch	43	3	Lawson et al., 1952
		Fibre insulation board	1/2 inch	58	2	Lawson et al., 1952
Proc. wood	Fibre reinf. panel	Fibre reinforced panel		20	141	Luzik, 1988
		Fibre reinforced panel		30	55	Luzik, 1988
		Fibre reinforced panel		40	33	Luzik, 1988
		Fibre reinforced panel		50	22	Luzik, 1988
		Fibre reinforced panel		60	15	Luzik, 1988
Asphalt	Asphalt	Asphalt shingles		12.6	906	Moysey et al., 1968
		Asphalt shingles		12.9	769	Moysey et al., 1968
		Asphalt shingles		13.5	326	Moysey et al., 1968
		Asphalt shingles		14.1	235	Moysey et al., 1968
		Asphalt shingles		14.7	206	Moysey et al., 1968
		Asphalt shingles		15	187	Moysey et al., 1968
		Asphalt shingles		15.9	158	Moysey et al., 1968

Class	Material group	Material	Details	Heat flux [kW/m^2]	Time to ignition [s]	Reference
		Asphalt shingles		18	139	Moysey et al., 1968
		Asphalt shingles		19.6	114	Moysey et al., 1968
Cloth	Wool	Wool	Carpet	58	26	Hilado, 1998
		Wool	Carpet	81	9	Hilado, 1998
		Wool	Carpet	105	6	Hilado, 1998
Cloth	Cotton	Cotton	Clothing	58	10	Hilado, 1998
		Cotton	Clothing	81	6	Hilado, 1998
		Cotton	Clothing	105	3	Hilado, 1998
Paint	Paint on wood	Red oil (Cedar)		16.1	848	Moysey et al., 1968
		Red oil (Cedar)		16.4	277	Moysey et al., 1968
		Red oil (Cedar)		17.1	243	Moysey et al., 1968
		Red oil (Cedar)		17.5	400	Moysey et al., 1968
		Red oil (Cedar)		18	193	Moysey et al., 1968
		Red oil (Cedar)		19.9	139	Moysey et al., 1968
		White enamel (Cedar)		16.7	1068	Moysey et al., 1968
		White enamel (Cedar)		17	611	Moysey et al., 1968
		White enamel (Cedar)		17.7	306	Moysey et al., 1968
		White enamel (Cedar)		20	220	Moysey et al., 1968
		White latex (Cedar)		16.1	1140	Moysey et al., 1968
		White latex (Cedar)		16.7	877	Moysey et al., 1968
		White latex (Cedar)		16.9	630	Moysey et al., 1968
		White latex (Cedar)		17.1	306	Moysey et al., 1968
		White latex (Cedar)		17.5	373	Moysey et al., 1968
		White latex (Cedar)		18.3	250	Moysey et al., 1968
		White latex (Cedar)		19.6	200	Moysey et al., 1968
		White oil (Cedar)		16.1	1808	Moysey et al., 1968
		White oil (Cedar)		16.7	936	Moysey et al., 1968
		White oil (Cedar)		17.1	821	Moysey et al., 1968
		White oil (Cedar)		17.4	485	Moysey et al., 1968

Class	Material group	Material	Details	Heat flux [kW/m^2]	Time to ignition [s]	Reference
		White oil (Cedar)		18	175	Moysey et al., 1968
		White oil (Cedar)		19.8	164	Moysey et al., 1968
Paint	Paint on wood	Dulux Gloss (Chipboard)		35	60	Staggs, 2003
		Dulux Gloss (Chipboard)		35	75	Staggs, 2003
		Dulux Gloss (Chipboard)		35	130	Staggs, 2003
		Dulux Gloss (Chipboard)		35	140	Staggs, 2003
		Dulux Gloss (Chipboard)		35	160	Staggs, 2003
		Dulux Gloss (Chipboard)		35	155	Staggs, 2003
		Dulux Gloss (Chipboard)		35	90	Staggs, 2003
		Dulux Gloss (Chipboard)		35	85	Staggs, 2003
		Dulux Gloss (Chipboard)		35	15	Staggs, 2003
		Dulux Gloss (Chipboard)		35	10	Staggs, 2003
		Dulux Gloss (Chipboard)		50	25	Staggs, 2003
		Dulux Gloss (Chipboard)		50	35	Staggs, 2003
		Dulux Gloss (Chipboard)		50	35	Staggs, 2003
		Dulux Gloss (Chipboard)		50	42	Staggs, 2003
		Dulux Gloss (Chipboard)		50	35	Staggs, 2003
		Dulux Gloss (Chipboard)		50	38	Staggs, 2003
		Dulux Gloss (Chipboard)		50	8	Staggs, 2003
		Dulux Gloss (Chipboard)		50	32	Staggs, 2003
		Dulux Gloss (Chipboard)		50	5	Staggs, 2003
		Dulux Gloss (Chipboard)		50	5	Staggs, 2003
		Dulux Gloss (Chipboard)		65	20	Staggs, 2003
		Dulux Gloss (Chipboard)		65	27	Staggs, 2003
		Dulux Gloss (Chipboard)		65	22	Staggs, 2003
		Dulux Gloss (Chipboard)		65	5	Staggs, 2003
		Dulux Gloss (Chipboard)		65	3	Staggs, 2003
		Dulux Gloss (Chipboard)		65	3	Staggs, 2003
		Dulux Gloss (Chipboard)		65	3	Staggs, 2003

Class	Material group	Material	Details	Heat flux [kW/m^2]	Time to ignition [s]	Reference
		Dulux Gloss (Chipboard)		65	3	Staggs, 2003
Paint	Paint on wood	Dulux Gloss (Plywood)		35	75	Staggs, 2003
		Dulux Gloss (Plywood)		35	85	Staggs, 2003
		Dulux Gloss (Plywood)		35	145	Staggs, 2003
		Dulux Gloss (Plywood)		35	230	Staggs, 2003
		Dulux Gloss (Plywood)		35	115	Staggs, 2003
		Dulux Gloss (Plywood)		35	97	Staggs, 2003
		Dulux Gloss (Plywood)		35	105	Staggs, 2003
		Dulux Gloss (Plywood)		35	85	Staggs, 2003
		Dulux Gloss (Plywood)		35	50	Staggs, 2003
		Dulux Gloss (Plywood)		50	35	Staggs, 2003
		Dulux Gloss (Plywood)		50	35	Staggs, 2003
		Dulux Gloss (Plywood)		50	70	Staggs, 2003
		Dulux Gloss (Plywood)		50	82	Staggs, 2003
		Dulux Gloss (Plywood)		50	74	Staggs, 2003
		Dulux Gloss (Plywood)		50	5	Staggs, 2003
		Dulux Gloss (Plywood)		50	45	Staggs, 2003
		Dulux Gloss (Plywood)		50	8	Staggs, 2003
		Dulux Gloss (Plywood)		50	10	Staggs, 2003
		Dulux Gloss (Plywood)		65	17	Staggs, 2003
		Dulux Gloss (Plywood)		65	45	Staggs, 2003
		Dulux Gloss (Plywood)		65	40	Staggs, 2003
		Dulux Gloss (Plywood)		65	33	Staggs, 2003
		Dulux Gloss (Plywood)		65	40	Staggs, 2003
		Dulux Gloss (Plywood)		65	5	Staggs, 2003
		Dulux Gloss (Plywood)		65	5	Staggs, 2003
		Dulux Gloss (Plywood)		65	5	Staggs, 2003

12 References

1. *Besluit kwaliteit leefomgeving (Bkl), Staatsblad van het Koninkrijk der Nederlanden 2018 292, https://wetten.overheid.nl/BWBR0041313/2024-01-01*. 2018.
2. A.M.C. Boxman, et al., *Advies aandachtsgebieden: Beschouwing van voorstel alternatieve benadering voor de berekening van aandachtsgebieden*, 2022-0012, 2022.
3. *PGS1, deel 1A: Effecten van brand op personen*, 2005.
4. *PGS1, deel 1B: Effecten van brand op constructies*, 2005.
5. *PIPESAFE collaboration Definition of house burning distance for public domain document*, PG/18/12, 2018.
6. M. Bilo and P.R. Kinsman, *Thermal radiation criteria used in pipeline risk assessment.* Pipes and Pipelines International, 1997(November-December).
7. J.C. Hazebroek, et al., *'Het kan verkeren' – Beschrijvend onderzoek naar brandontwikkeling en overleefbaarheid*, 2015.
8. G. Burrell and J. Hare, *Review of HSE Building Ignition Criteria*, HSL/2006/33, 2006.
9. R.E. Lyon and J.G. Quintiere, *Criteria for piloted ignition of combustible solids.* Combustion and Flame, 2007. **151**(4): p. 551-559.
10. M.J. DiDomizio, P. Mulherin, and E.J. Weckman, *Ignition of wood under time-varying radiant exposures.* Fire Safety Journal, 2016. **82**: p. 131-144.
11. I. Vermesi, et al., *Pyrolysis and ignition of a polymer by transient irradiation.* Combustion and Flame, 2016. **163**: p. 31-41.
12. J. Panagiotou. *A Methodology for Flammability Diagrams*. PhD thesis. University of Maryland, 2004.
13. W. An, et al., *Correlation analysis of sample thickness, heat flux, and cone calorimetry test data of polystyrene foam.* Journal of Thermal Analysis and Calorimetry, 2015. **119**(1): p. 229-238.
14. B. Moghtaderi, et al., *A new correlation for bench-scale piloted ignition data of wood.* Fire Safety Journal, 1997. **29**(1): p. 41-49.
15. X. Zhang, et al., *Experimental study of commercial flame-retardant polycarbonate under external heat flux: Ignition time and mass loss rate.* Journal of Thermal Analysis and Calorimetry, 2018. **131**(2): p. 1463-1470.
16. M.M. Khan, J.L. De Ris, and S.D. Ogden. *Effect of moisture on ignition time of cellulosic materials*, Fire Safety Science. pp. 167-178. 2008.
17. M.J. Spearpoint and J.G. Quintiere, *Predicting the piloted ignition of wood in the cone calorimeter using an integral model - Effect of species, grain orientation and heat flux.* Fire Safety Journal, 2001. **36**(4): p. 391-415.
18. N. Safronava, et al., *Effect of Moisture on Ignition Time of Polymers.* Fire Technology, 2014. **51**(5): p. 1093-1112.
19. G.W.H. Silcock and T.J. Shields, *A protocol for analysis of time-to-ignition data from bench scale tests.* Fire Safety Journal, 1995. **24**(1): p. 75-95.
20. D.I. Lawson and D.L. Simms, *The ignition of wood by radiation.* British Journal of Applied Physics, 1952. **3**.

21. R. Bilbao, et al., *A model for the prediction of the thermal degradation and ignition of wood under constant and variable heat flux.* Journal of Analytical and Applied Pyrolysis, 2002. **62**(1): p. 63-82.
22. M.A. Azhakesan, T.J. Shields, and G.W.H. Silcock, *On the nature, influence and magnitudes of flame heat transfer during surface flame spread.* Fire Safety Journal, 2000. **35**(3): p. 189-222.
23. B.T. Rhodes and J.G. Quintiere, *Burning rate and flame heat flux for PMMA in a cone calorimeter.* Fire Safety Journal, 1996. **26**(3): p. 221-240.
24. J.E.J. Staggs, H.N. Phylaktou, and R.E. McCreadie, *The Effect of Paint on the Ignition Resistance of Plywood and Chipboard.* Fire Safety Science, 2003. **7**: p. 617-628.
25. E.B. Moysey and W.E. Muir, *Pilot ignition of building materials by radiation.* Fire Technology, 1968. **4**: p. 46-50.
26. C.R. Harris, et al., *Array programming with NumPy.* Nature, 2020. **585**(7825): p. 357-362.
27. P. Virtanen, et al., *SciPy 1.0: fundamental algorithms for scientific computing in Python.* Nat Methods, 2020. **17**(3): p. 261-272.
28. *Pacific Gas and Electric Company Natural Gas Transmission Pipeline Rupture and Fire, San Bruno, California, September 9, 2010*, PAR-11/01, 2011.
29. *Columbia Gas Transmission Corporation Pipeline Rupture, Sissonville, West Virginia, December 11, 2012*, PAR-14/01, 2014.
30. *Schwere Gasexplosion in Ludwigshafen-Oppau*. Available via https://www.mannheim24.de/region/fotostrecke-schwere-explosion-ludwigshafen-oppau-vermutlich-gasexplosion-4221487.html. (Accessed on 2023-08-15).
31. R. Eichelsheimer. *Die Katastrophe aus der Vogelperspektive*. Available via https://www.ludwigshafen24.de/region/ludwigshafen-oppau-luftbilder-gasexplosion-ludwigshafen-4317392.html. (Accessed on 2023-08-15).
32. R. Eichelsheimer. *Schwere Gasexplosion in Ludwigshafen-Oppau*. Available via https://www.heidelberg24.de/region/ludwigshafen-oppau-gas-pipeline-explodiert-toter-verletzte-nach-schwerer-explosion-4225138.html. (Accessed on 2023-08-15).
33. P. Kiefer. *Zwei Tage nach Gas-Explosion: Großes Aufräumen in Oppau!* Available via https://www.ludwigshafen24.de/ludwigshafen/fotos-aufraeumarbeiten-nach-gas-explosion-ludwigshafen-oppau-einem-toten-4261955.html. (Accessed on 2023-08-15).
34. *Enbridge Inc. Natural Gas Transmission Pipeline Rupture and Fire, Danville, Kentucky, August 1, 2019*, PIR-22/02, 2022.
35. RIVM. *CAROLA quickstart*. Available via https://www.rivm.nl/documenten/omgevingsveiligheid/carola-quickstart. (Accessed on 2025-01-20).
36. R. Bilbao, et al., *Experimental and theoretical study of the ignition and smoldering of wood including convective effects.* Combustion and Flame, 2001. **126**(1-2): p. 1363-1372.
37. R. Chen, et al., *Correlation analysis of heat flux and cone calorimeter test data of commercial flame-retardant ethylene-propylene-diene monomer (EPDM) rubber.* Journal of Thermal Analysis and Calorimetry, 2016. **123**(1): p. 545-556.

38. M. Delichatsios, B. Paroz, and A. Bhargava, *Flammability properties for charring materials.* Fire Safety Journal, 2003. **38**(3): p. 219-228.
39. M.A. Delichatsios, *Piloted ignition times, critical heat fluxes and mass loss rates at reduced oxygen atmospheres.* Fire Safety Journal, 2005. **40**(3): p. 197-212.
40. A. Gibson, et al., *Fire Performance of Composite Materials for Offshore Use, Composite Materials for Offshore Use.* I Mech E, 1994.
41. J. Hallman, J. Reed Welker, and C.M. Sliepcevich, *Ignition of Polymers.* SPE Journal, 1972. **28**.
42. C.J. Hilado, *Flammability Handbook for Plastics* 5th, ed., 1998.
43. S.J. Luzik, *Fire and Explosion Investigation, Pacific Engineering and Production Co. of Nevada*, 1988.
44. H.E. Thomson and D.D. Drysdale, *Flammability of plastics I: Ignition temperatures.* Fire and Materials, 1987. **11**(4): p. 163-172.
45. D.D. Drysdale and H.E. Thomson, *Flammability of plastics II: Critical mass flux at the firepoint.* Fire Safety Journal, 1989. **14**(3): p. 179-188.
46. H.R. Wesson, J.R. Welker, and C.M. Sliepcevich, *The piloted ignition of wood by thermal radiation.* Combustion and Flame, 1971. **16**(3): p. 303-310.
47. L. Yang, et al., *The pyrolysis and ignition of charring materials under an external heat flux.* Combustion and Flame, 2003. **133**(4): p. 407-413.

Published by:

National Institute for Public Health and the Enviroment, RIVM
P.O. Box 1 | 3720 BA Bilthoven
The Netherlands
www.rivm.nl/en

April 2025

Committed to
health and sustainability